MOLECULAR MECHANISMS UNDERLYING THE NEUROPROTECTIVE EFFECTS OF AAA ATPase THORASE

by

Leire Abalde-Atristain

A dissertation submitted to Johns Hopkins University in conformity with the requirements for the degree of Doctor of Philosophy.

Baltimore, Maryland

May, 2019

Abstract

Diseases that affect the nervous system represent a great burden to society. Given the diverse etiology, designing neuroprotective strategies would provide a common therapeutic alternative for the prevention and treatment of these neurological conditions. In an attempt to understand the intrinsic mechanisms the brain possesses to maintain homeostasis and promote cell survival, our laboratory had previously discovered the AAA+ ATPase, Thorase. Using energy from ATP hydrolysis, Thorase regulates neuronal excitability through the internalization of AMPA receptors, and it maintains mitochondrial and peroxisomal integrity by extracting mislocalized proteins out of these organelles. Since the family of AAA+ ATPases is known for associating with diverse cellular functions, and the clinical manifestation of emerging pathogenic Thorase variants is miscellaneous, elucidating additional Thorase functions would help us better understand its neuroprotective effects and harness its therapeutic potential.

In this study, we uncovered a novel role for Thorase in regulating mechanistic target of rapamycin complex 1 (mTORC1) signaling. We have shown that Thorase directly binds mTOR, thereby orchestrating the disassembly of the mTORC1. In the absence of Thorase, mTORC1 signaling and downstream processes were upregulated. Importantly, the mTORC1 hyperactivity observed in the absence of Thorase could be alleviated through the FDA-approved mTOR inhibitor rapamycin. Moreover, rapamycin substantially prolonged survival of mice lacking Thorase, which typically die of severe seizures shortly after birth. Collectively, these findings revealed a key role for Thorase as negative regulator of the mTORC1 signaling pathway that acts through the disassembly

of the mTORC1, thereby suggesting Thorase neuroprotective effects rely on maintaining neurons in a bioenergetically favorable state.

(Readers: Valina L. Dawson, Ph.D. and Philip C. Wong, Ph.D.)

Acknowledgments

First of all, I would like to thank the Cellular and Molecular Medicine program for giving me the outstanding opportunity to conduct my graduate studies at Johns Hopkins University School of Medicine. This training opportunity could also have not been possible without the La Caixa Foundation, which supported my stipend and tuition for the first two years.

I am most grateful to my advisors Valina and Ted Dawson for their unconditional support and trust. Their laboratory has been the ideal niche to grow as independent scientist, and I have felt truly privileged being part of a team of researchers who are moving the field of neurodegeneration forward. Ted and Valina have always backed my career choices, including an internship with the wonderful editorial team led by Dr. Orla Smith at *Science Translational Medicine*. This memorable career opportunity was conceived with the kind help of Caroline Pounds from the Biomedical Careers Initiative.

I am very lucky that my thesis committee members – Drs. Philip Wong, Paul Worley, Jay Baraban and Tom Lloyd –vouched for my timely graduation and provided insightful advice for my projects. I am particularly thankful to Dr. Wong, who kindly accepted to chair the committee throughout the years and read my dissertation.

I am thankful to our collaborators from the laboratories of Drs. Taekjip Ha and Paul Worley, as well as from the Microscope Facility, who took our research in very

interesting and fruitful directions. My research rotation mentors, Drs. Linzhao Chen and Hongjun Song, also gave me the chance to participate in interesting research projects.

During my time in the Dawson laboratory, I have had the fortune to learn from and work with excellent investigators. Dr. Ian Martin instructed me on many useful benchtop techniques and helped develop my ability to design and think critically about research. Dr. George Umanah was a delight to work with, and I am grateful for his patience, positivity and for having learnt from his biochemistry wisdom. Dr. Senthil Karuppagounder taught me all about mouse work and was an example of hard work. Drs. Stephen Eacker, Repon Khan, Xiling Yin and Agnes Lau inspired me to be rigorous, meticulous and creative. Dr. Wren Kim was the model graduate student that I have strived to become for my juniors Laura Scott, Aanisha Jhaldiyal and Jared Hinkle, with whom the learning process has actually gone both ways. Eleni Georgantonis and Stewart Neifert have helped me and other lab mates in many ways and, to me, embody the laboratory's collegiality.

On a personal note, I have to thank my mother for always encouraging me to take the career opportunities she never had, and for being my number one cheerleader. Although my father died many years ago, I try to honor his memory by deeply caring about my friends, just as people say he did. My sister taught me that doing what you are passionate about can take you far, and this is something that I really held onto when facing frustration and failure. Also, she has recently endowed me with the joy of being Telmo's aunt.

Aside from the privilege of conducting cutting-edge, curiosity-driven, bedside-oriented research, one of the best things about my time at Hopkins is the many exceptional human beings that I had the chance to meet. I must single out Adeline Yong, whom I met as classmate but now consider a non-blood sister. Last but not least, during these final months as PhD candidate, I have enjoyed the most supportive companionship from my partner Ian, with whom I am perfectly and incandescently happy to share this career milestone.

Table of Contents

List of Figures

Chapter 1. Introduction

According to estimates from the World Health Organization, neurological disorders including epilepsy and stroke constitute 6.3% of the global disease burden, a contribution steadily increasing when one compares past and future projections (years 2005 and 2015 *versus* 2030). Among neurological disorders, over half of the burden in disability-adjusted life years, a quantifiable measure for lost years of healthy life, is attributable to cerebrovascular disease, 12% to Alzheimer's disease and other dementias and 8% to epilepsy. Neurological disorders are also a major cause of mortality and contribute to 12% of total deaths globally, with cerebrovascular diseases accountable for 85% of these.

Diverse molecular mechanisms underlie different neurological diseases that result in alteration of particular brain circuits or the death of specific neuronal populations. Accordingly, extensive research efforts are directed to the identification and understanding of disease-specific agents and mechanisms, with the aim of identifying druggable targets that may be approached in the clinic. For instance, researchers in the field of Parkinson's disease aim to comprehend how alpha-synuclein aggregates and spreads throughout the brain, and investigators working on epilepsy seek to find the causes for excess brain excitability that underlie seizures.

Finding specific disease-modifying therapeutic interventions is desirable. Alternatively, designing neuroprotective strategies would provide common therapeutic ground for the prevention and treatment of pathologically diverse degenerative processes. To enable this, it is crucial to dissect the intrinsic mechanisms the brain possesses to maintain

homeostasis and promote cell survival. Given the high metabolic demands of the brain, it will be especially interesting to lay out the principles that maintain neurons in a bioenergetically favorable state.

AAA+ ATPase Thorase

Discovery of the neuroprotective gene encoding for Thorase

Preconditioning refers to the capacity of the nervous system to activate signaling pathways that promote cell survival upon sub-lethal insults, that prepare it for potential subsequent damaging episodes (Gidday, 2006). Using oxygen/glucose deprivation (OGD) and N-methyl-D-aspartate (NMDA) treatments to induce preconditioning *in vitro*, Dai and colleagues screened for genes that could confer neuroprotection in primary cortical neurons derived from rats (Dai et al, 2010). Twenty-eight genes were discovered and validated for their ability to prevent neuronal death against lethal OGD or NMDA treatment, among which was a gene of unknown function, AAA domain containing 1 (*ATAD1*), a putative AAA+ ATPase. *ATAD1* was re-named as *Thorase*, after the Norse god of thunder and lightning, Thor (Dai et al, 2010).

Superfamily of AAA+ ATPases

AAA+ ATPases (ATPases associated with diverse cellular activities) comprise of a large family of highly-conserved proteins found in all kingdoms of life (Hanson & Whiteheart, 2005). AAA+ ATPases are referred to as "molecular motors" because they function analogously to an engine, transforming the chemical energy from ATP hydrolysis into mechanic force that induces an initial conformational change in the active site, which

then propagates to distal subunits of the protein and then further to its interacting proteins. The conformational changes stemming from repeated cycles of ATP hydrolysis thus enable AAA+ ATPases to execute and participate in a myriad of functions, from protein unfolding, disaggregation and complex disassembly, to membrane trafficking, proteolysis or DNA replication.

Among the extensively-characterized AAA+ ATPases, p97 exemplifies the versatility of the proteins within this family well (Stach & Freemont, 2017). p97 governs diverse functions in the cell, including membrane fusion, endoplasmic reticulum-associated degradation or NF-kappaB (nuclear factor kappa-light-chain enhancer of activated B cells) activation, among others. The functional ubiquity of 97 is enabled by its association with a multitude of adaptor proteins and cofactors that shuttle and assist it at different subcellular locations and with various substrates. At a specific site of action, p97 harnesses the energy from ATP hydrolysis to extract and shuttle a given substrate from a cellular structure or complex for degradation. Unsurprisingly, mutations in p97 have been linked to clinically diverse neurodegenerative conditions, such as inclusion body myopathy, frontotemporal dementia, Amyotrophic Lateral Sclerosis (Johnson et al, 2010) or Parkinson's disease (Tang & Xia, 2016).

AAA+ ATPases are characterized by a core ATP-binding domain spanning 200-250 amino acids. This domain contains the Walker A and B motifs, which are critical for binding and hydrolyzing ATP (Miller & Enemark, 2016). ATP hydrolysis depends on a conserved glutamate residue within the Walker B motif and mutation of this residue to

alanine therefore prevents ATP hydrolysis while still allowing for ATP binding. As ATP is required for substrate binding by most AAA+ proteins, Walker B mutants behave as "substrate traps" that bind but will not release substrates. Similarly, non-hydrolyzable ATP maintain AAA+ ATPases in the oligomeric substrate-bound state. In contrast, mutation of a conserved lysine residue within the Walker A motif disrupts ATP binding, therefore interfering with substrate binding (Hanson & Whiteheart, 2005).

Members of the AAA+ ATPase family often assemble into oligomers with ATPase sites located at the interfaces of neighboring subunits, with adjacent subunits contributing residues to a bipartite active site (Sysoeva, 2017). While initial structural studies indicated that most AAA+ ATPases oligomerize into symmetrical hexameric rings, recent advances in structural techniques have evidenced that diversity also governs the arrangement of AAA+ ATPases. These alternative oligomeric structures include pentamers (clamp loader), heptamers (NtrC1), octamers (CED-4), helical filaments (DnaA) and non-symmetrical hexamers (NSF) (Sysoeva, 2017).

The large scope of human diseases associated with AAA+ ATPases underscore their relevance in maintaining normal physiology. Aside from the maladies linked to p97 mutations mentioned earlier, mutations in AAA+ ATPases involved in peroxisomal protein import underlie Zellweger's type peroxisome-biogenesis disorders, a type of leukodystrophy with loss of myelin, the first AAA+ ATPase disease to be identified (Reuber et al, 1997). Torsin A, which resides in the lumen of the endoplasmic reticulum, is mutated in early-onset dystonia (Goodchild & Dauer, 2004). Aberrancies in Katanin, a

AAA+ protease that severs microtubules, causes hereditary spastic paraplegia (Evans et al, 2005).

Structure and conservation of Thorase

Since the discovery of Thorase as neuroprotective protein presenting homology to AAA+ ATPases, several studies have sought to characterize its structure, function and conservation across phyla.

In humans, the gene for Thorase is located on the long arm of chromosome 10 (10q23.31). It encodes for a protein of 361 amino acids, with molecular weight of approximately 41 kDa. The protein contains a transmembrane domain at the N-terminal end and a highly conserved AAA+ domain toward the C-terminal end (Figure 1-1).

Functions of Thorase unraveled heretofore

<u>Thorase orchestrates the removal of AMPAR from postsynaptic membranes</u>

In a landmark Thorase study published in 2011, Zhang and colleagues explored the distribution of Thorase in different tissues. They detected highest expression in brain and testes. Within the brain, Thorase expression levels were found to be heterogenous, with pyramidal cells in the CA1 region of the hippocampus expressing it in relatively high levels (Zhang et al, 2011). Subcellularly, Thorase was enriched at synapses and co-localized with postsynaptic markers like PSD95.

In postsynaptic membranes, presence of the ionotropic glutamate α-amino-3-hydroxy-5-methyl-4-isoxazolepropionic acid receptor (AMPAR) partially determines the strength of a synapse, and neuronal excitability can be controlled by regulating the insertion or removal of these receptors (Moretto & Passafaro, 2018). Through a series of biochemical, imaging and electrophysiological experiments, the authors demonstrated that Thorase facilitates the endocytosis of GluA2 subunit-containing AMPARs from synapses. ATP binding and hydrolysis were necessary for Thorase to disassemble GluA2 subunits from GRIP1 at postsynaptic membranes (Figure 1-2A).

The whole-body homozygote Thorase knockout mice created for this study were viable but approximately 80% died of a seizure-like syndrome within 3 weeks after birth, and were significantly smaller in size than their wild type littermates since birth. Heterozygous knockout mice showed no obvious developmental or behavioral abnormalities and were viable. Mice lacking Thorase had increased postsynaptic AMPARs without an alteration in AMPAR subunit composition, with consequent increases in AMPA but not NMDA postsynaptic currents. Primary cortical neuron cultures from these mice presented with higher baseline levels of surface AMPAR that could further be increased with tetradotoxin, while their bicuculline-induced internalization was impaired, indicating an impediment of AMPAR endocytosis, but not insertion. These defects could be reduced by heterologous expression of Thorase. Behaviorally, this excess AMPAR maintenance at the synapses resulted in enhanced long-term potentiation and impaired long-term depression of synapses, with profound effects on learning and memory.

A study published shortly after suggested a possible regulation of the interaction between Thorase and other AMPAR-trafficking complexes (ATCs) by gangliosides (Prendergast et al, 2014). Specifically, this study found that while GluA2 binds selectively to ganglioside GM1, Thorase and other ATC proteins bind ganglioside GT1b, through the adapter protein Nicalin, potentially keeping these components physically separated as a means to control AMPAR endocytosis. *In vivo*, mice carrying mutations in ganglioside biosynthesis enzymes found in human congenital disorders with early onset seizures have altered ganglioside membrane compositions, and AMPAR and ATC binding dynamics.

Thorase participates in the quality and control of mitochondria and peroxisomes

In a radically different set of discoveries, Thorase emerged as an important component in the maintenance of healthy peroxisomes and mitochondria. In a pair of back-to-back publications, Thorase and its yeast homolog Msp1 were found to be required to prevent the aberrant accumulation of a subset of proteins, the tail-anchored (TA) proteins, in the mitochondria, thereby maintaining mitochondrial health and integrity (Chen et al, 2014; Okreglak et al, 2014) (Figure 1-2B). These composite of research studies show the high degree of functional conservation of Thorase in yeast, flies and mammals (Figure 1-1).

Tail-anchored proteins are post-translationally chaperoned to either mitochondria or the endoplasmic reticulum, from where they are subsequently shuttled into other membrane compartments such as the peroxisome, by a dedicated system called the Guided Entry of Tail-anchored proteins (GET).

Loss of yeast Msp1, which was otherwise found to be integrally embedded in the outer mitochondrial membrane, led to the accumulation of the peroxisomal TA protein Pex15 in mitochondria, which was exacerbated upon deletion of GET proteins. Steady state levels of Pex15 were higher and its degradation rate slower in the absence of Msp1, indicating that Msp1 promotes the degradation of mislocalized proteins concomitant to their extraction from their non-cognate organelles. In support of this, Msp1 and Pex15 were proven to physically interact. These observations were validated with the human homologs, ATAD1 and PEX26.

Besides the accumulation of mislocalized TA proteins, the brains of Thorase knockout mice have lower levels of several mitochondrial proteins and reduced respiratory mitochondrial capacity, alongside with aberrant mitochondrial morphology and fragmentation. Loss of Msp1 also induced a failure to grow on certain carbon sources, a phenotype that could be partially rescued by ectopic expression of the *Drosophila melanogaster* homolog Dmel\nmd.

Two subsequent studies aimed to gain further insight into how Msp1 may extract mislocalized TA proteins from mitochondria. Wohlever and colleagues showed, using *in vitro* reconstituted proteoliposomes, that Msp1 alone could extract TA proteins from the membrane in an ATP-dependent manner, without the assistance of any other factors. Crystal structure of the cytosolic end of Msp1 revealed a ring-shaped hexamer with a central pore facing the membrane. Mutations of pore-forming residues or mutations that

impeded the ring formation disrupted the ability of Msp1 to extract proteins from the liposomes (Wohlever et al, 2017). In the more recent publication authored by Li and colleagues, the mechanism by which Msp1 recognizes mislocalized TA proteins was proposed. Presumably, mislocalized TA proteins expose hydrophobic surfaces, which Msp1 can detect through its N-domain. This recognition triggers the rearrangement of Msp1 monomers into active hexamers that can hydrolyze ATP to dislocate the substrate (Li et al, 2019). Although the membrane extraction function of Msp1 seems to be conserved in mammals, it will be interesting to see whether these findings are applicable to Thorase/ATAD1.

A study conducted by Liu and colleagues showed that Thorase is targeted to peroxisomes and suggested that it may perform a quality and control function there similar to the one described in mitochondria (Liu et al, 2016).

Emerging importance of Thorase in human disease

In 2017, the first pathogenic variant of human Thorase was reported in a consanguineous Kuwaiti family with multiple newborns suffering from seizures, encephalopathy, hypertonia and respiratory failure that led to early death (Ahrens-Nicklas et al, 2017).

Pedigree analysis suggested an autosomal recessive inheritance pattern, and exome sequencing followed by single nucleotide polymorphism analysis linked a novel homozygous variant of Thorase to the affected probands, which was carried by the unaffected parents. This homozygous transversion (826 G>T) predicted a substitution of

a glutamic acid residue to a premature stop codon (E276X). In lymphoblasts from patients, Thorase mRNA levels were greatly decreased and Thorase protein was undetectable by Western blotting, reportedly because the early polypeptide termination would trigger the degradation of mRNA through nonsense-mediated decay.

Consistent with a potential pathogenic loss-of-function conferred by this novel human variant, there was overlap between the clinical manifestation of the affected neonates and the phenotype of homozygous Thorase knockout mice, including seizures and early death (Zhang et al, 2011). Based on this resemblance, and the known role of Thorase in AMPAR recycling, it was postulated that the FDA (Food and Drug Administration)-approved AMPAR antagonist, Perampanel, may provide therapeutical benefit in Thorase-deficient mice and newborns carrying loss-of-function Thorase variants.

Treatment of Thorase knockout mice with Perampanel decreased the excess spontaneous locomotor activities and extended their survival, while off-label compassionate treatment of affected individuals with Perampanel resulted in an improvement in the tone in patients and stopped seizures. One of the probands had severe neurological symptoms at the time he was treated with Perampanel, at 16 months of age. While his hydrocephalus (accumulation of cerebrospinal fluid) continued worsening, Perampanel improved his tone and reflexes including his pupillary response to light, while his brain activity monitored via electroencephalogram (EEG) normalized. A cousin of this patient was treated early at 2.5 months of age, before her neurological functions had severely declined. Perampanel improved her hypertonia, normalized her EEG activity and she

maintained some basic responses such as the brain stem reflexes, the ability to vocalize pain and her spontaneous limb movements.

Prior to this seminal study on a pathogenic mutation in *Thorase/ATAD1*, the gene was not known to be associated with human disease. Within 2 years from this case report, additional families have been identified that carry pathogenic variants in Thorase. Collectively, Thorase mutations are currently categorized by the Online Mendelian Inheritance in Man database under a hyperekplexic phenotype, or congenital stiff-baby syndrome (OMIM entry # 618011). The severity of the clinical cases underscores the pivotal role of Thorase in maintaining normal physiology, especially in the brain, while the broad clinical manifestations grant further research to elucidate whether different and yet unknown functions of Thorase may be responsible for the pathological discrepancies.

Mechanistic Target of Rapamycin kinase

mTOR (mechanistic Target Of Rapamycin) is a highly conserved kinase that links the growth, survival, division, migration and differentiation of cells to the availability of nutrient and growth factors in the environment that they are in. mTOR does so by acting as master switch that balances the activation of energy-producing and -consuming metabolic activities. mTOR is a central signaling hub in cells and, as such, a wide range of human diseases have been attributed to aberrant function of its pathway.

Discovery of mTOR

In the 1960s, a group of expeditioners collected soil samples in the Chilean Easter Island (also known as Rapa Nui), in search for novel antimicrobial compounds. Among these they found the eponymous macrolide, rapamycin, which they isolated from *Streptomyces hygroscopicus* and possessed potent antifungal, antitumoral and immunosuppressive effects (Vézina et al, 1975; Martel et al, 1977; Eng et al, 1984).

In parallel efforts to identify the cellular target of rapamycin, genetic screens in yeast and biochemical approaches in mammals led to the discovery of the Target of Rapamycin (TOR), a highly conserved serine/threonine kinase with homology to the PI3K-related protein kinases (PIKKs) (Koltin et al, 1991; Heitman et al, 1991; Sabatini et al, 1994; Brown et al, 1994; Sabers et al, 1995). Rapamycin binds and inhibits mTOR allosterically in complex with FKBP12.

In the 25 years since its discovery, tremendous progress has been made to elucidate the molecular and biochemical mechanisms centered around mTOR, including cofactors, downstream kinase targets, the biochemical processes regulated by these phosphorylation events, and the cues and molecular stakeholders that activate and inhibit the pathway (Sabatini, 2017; Valvezan & Manning, 2019).

mTOR signaling pathway

mTOR is the catalytic component of two functionally distinct macromolecular complexes, the mTOR complex 1 (mTORC1) and the mTORC2. Raptor (Regulatory associated protein of mTOR) and Rictor (Rapamycin-insensitive companion of mTOR)

are defining protein components of mTORC1 and mTORC2, respectively, and are thought to enable mTOR kinase activity by acting as scaffolds for recruiting mTOR substrates (Hara et al, 2002; Kim et al, 2002, Sarbassov et al, 2004).

Comparably much less is known about the mTORC2, which through the activation of the PI3K/AKT signaling pathway controls the arrangement of the actin cytoskeleton and plays a role in the survival, proliferation and migration of cells.

In contrast, mTORC1 has been studied in depth. mTORC1 activity stimulates metabolic processes that synthesize macromolecules (anabolic), while it inhibits those that lead to their breakdown (catabolic). For instance, mTORC1 induces protein synthesis via promoting the translation of specific mRNAs that encode for proteins of the translation machinery (5' terminal oligopyrimidine tract mRNAs), and by promoting ribosome biogenesis (Ma & Blenis, 2009). Among the translational kinase targets of mTORC1 are ribosomal S6 kinases (S6K) and the eukaryotic translation initiation factor 4E-binding proteins (4EBP). 4E-BP binding to eIF4E blocks the recruitment of the small ribosomal subunit to the mRNA 5' cap. mTOR phosphorylation of 4E-BP releases it from eIF4E, thereby allowing for translation initiation. S6K owes its name to its substrate ribosomal protein S6, although how this phosphorylation promotes translation remains a mystery. S6K also phosphorylates another eukaryotic initiation factor, eIF4B, which in turn stimulates the helicase activity of its partner eIF4A, leading to the translation of mRNAs with complex untranslated regions.

Ribosomes are large molecular machines where the catalytic component relies in the activity of RNAs. Therefore, an increase protein synthesis has to be accompanied with transcription of ribosomal RNAs and synthesis of nucleotide building blocks, both of which are also the result of mTOR activation (Iadevaia et al., 2014; Ben-Sahra et al, 2014; Robitaille et al, 2013). In parallel, mTORC1 also stimulates the synthesis of lipids through the activation of the Sterol Regulatory Element-Binding Protein (SREBP) family of transcription factors (Porstmann et al, 2008).

As mTORC1 becomes active, autophagy and lysosomal function, which are integral parts of the degradation machinery in the cell, arrests. mTORC1 accomplishes this by phosphorylating the autophagy-initiating kinase UNC-51-like kinase 1 (ULK1) and the transcription factor EB (TFEB), a master regulator of lysosome biogenesis (Egan et al, 2011; Peña-Llopis, 2011).

Regulation of mTORC1 activity

Recent studies have provided great mechanistic insight into where and how mTORC1 is activated (Valvezan & Manning, 2019). A small G protein, Rheb, can directly bind and activate mTORC1, potentially through conformational changes that activate the kinase activity of mTOR (Yang et al, 2017). Only when bound to GTP, but not GDP, Rheb can exert its activating effects on mTORC1. Therefore, the stimuli that impinge upon the activation state of mTORC1 converge in the regulation of the GTP/GDP-bound state of Rheb, through the tuberous sclerosis (TSC) complex, which comprise proteins TSC1, TSC2 and TBC1D7. TSC2 has a GTPase-activating protein (GAP) activity towards

Rheb, whereby it inactivates it (Figure 1-3A). Several kinases stimulated by either growth factors or different kinds of stress cues phosphorylate and influence the activity of the TSC complex, thereby connecting extracellular and intracellular signaling (Dibble & Manning, 2013).

A subpopulation of Rheb proteins can be found at the lysosome, where mTORC1 needs to be shuttled for activation. A pair of antagonizing small G protein heterodimers, the RagA/B and RagC/Ds proteins, are responsible for the regulated recruitment of mTORC1 to the lysosome through their interaction with Raptor (Sancak et al, 2008). Rag GTPases localize to the lysosome through yet another protein complex, the Ragulator (also known as LAMTOR) and a lysosomal amino acid transporter, SLC38A9 (Sancak et al, 2010). Similar to Rheb, the activity or Rag proteins is also regulated by their GTP/GDP-bound status, with RagA/Bs specifically active in the GTP-loaded state and Rag C/Ds active in the GDP-loaded state (Figure 1-3A). Therefore, modulating the nucleotide state of the Rag proteins impacts mTORC1 activation at the lysosome. The Rag protein nucleotide-loading regulation network is sensitive to intracellular amino acid levels, the building blocks for the synthesis of proteins, which is the most energy- and nutrient-demanding biosynthetic process. GAP activity toward Rags 1 (GATOR1) anchors to the lysosome through a protein complex called KICSTOR, and exerts its GAP activity towards RagA/B in the absence of amino acids, thereby preventing mTORC1 recruitment to the lysosome (Bar-Peled et al, 2013; Panchaud et al, 2013; Wolfson et al, 2017). GATOR1 can be inhibited by SAMTOR, which senses the levels of S-adenosylmethionine, a proxy for methionine levels in the cell (Gu et al, 2016). Another protein called GATOR2 can also

inhibit GATOR1, only in the presence of arginine and leucine, in which case GATOR2 is not sequestered by their respective protein sensors, CASTOR1 and Sestrin2 (Chantranupong et al, 2016; Wolfson et al, 2016).

In summary, both amino acid and growth factors are required for mTOR activation, a co-requisite which is integrated through the so-called AND-gate signaling, where the presence of amino acids allows GTP-bound RagA/Bs to recruit mTORC1 proximally to Rheb, which will in turn be GTP-loaded if growth factors stimulate the release of TSC complexes away from the lysosome (Menon et al, 2014) (Figure 1-3B).

While many details about how mTOR is activated at the lysosome are known, it is less clear where and how the complex gets inactivated. Given the different layers of regulation participating in the regulation of mTORC1 assembly and activation, it is reasonable to expect that the disassembly of the complex would also involve dedicated proteins that respond to nutrients, growth factors, energy levels or stress.

mTOR in disease

Given the central role of mTOR in the growth, metabolism and survival of cells, it is not surprising that dysregulation of the signaling pathway has been suggested to underlie radically disparate pathogenic processes, including cancer, diabetes to autism or Parkinson's disease (Saxton & Sabatini, 2017).

As one of the most energy-demanding organs in the body, the brain is particularly susceptible to metabolic dysregulation (Lipton & Sahin, 2014). In neurodegenerative processes, aberrant mTOR signaling may contribute in different ways. On one hand, excess mTOR activation could overshoot neurons with the demands of protein synthesis, which could saturate the chaperones that ensure proper protein folding. On the other hand, blockade of autophagy by active mTOR could impair the clearance of damaged organelles and protein aggregates. During development, incorrect migration or differentiation of neurons and failed synapse formation may subvert neural circuit formation.

A considerable amount of mutations in mTOR pathway components have been found in the particular case of epilepsies associated with malformations of cortical development, which have collectively been coined as "mTORophathies" (Crino, 2015). Mutations in several genes like TSC2, GATOR1 or mTOR itself in these epilepsies seem to all have in common that they lead to a hyperactivation of mTORC1, which may trigger onset of seizures due to abnormal arrangement of the cortical laminae, cell size and lineage commitment or impinging upon neuronal excitability itself (Crino, 2016; Baulac, 2016). Accordingly, the use of mTOR inhibitors has been explored in the clinic, with some promising results (Citraro, 2016).

Figure 1-1. Protein sequence alignment of Thorase homologues.

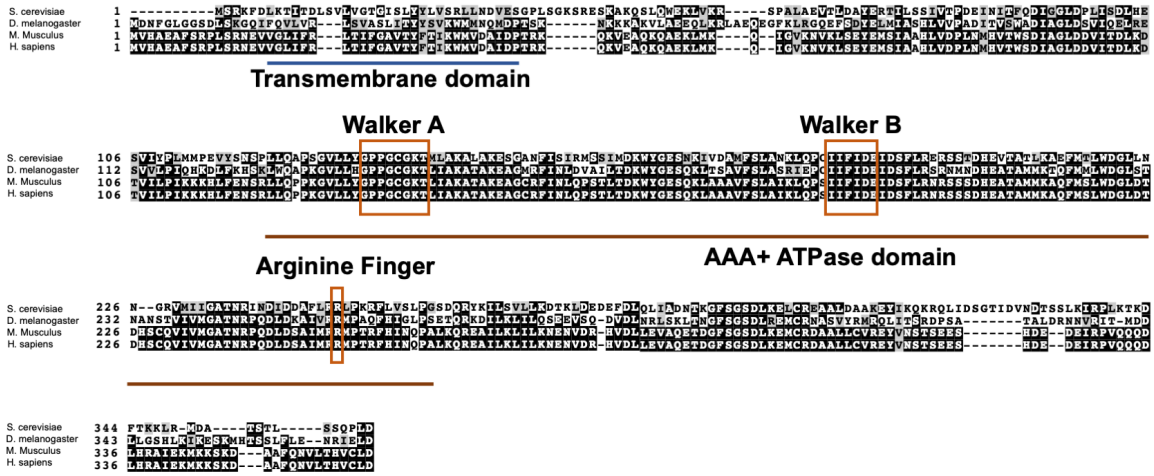

Figure 1-1. Protein sequence alignment of Thorase homologues. Protein sequence alignment of Thorase (*H. sapiens*) and its homologues, ATAD1 in mouse (*M. musculus*), Dmel\nmd in the fruit fly (*D. melanogaster*) and Msp1 in budding yeast (*S. cerevisiae*) aligned with ClustalW and rendered with Boxshade. Identical residues are highlighted in black and similar ones in gray. Residues within canonical AAA+ ATPase domains are shown in an orange box. The span of the ATPase domain is indicated with a brown line, and the domain in the N-terminus that anchors Thorase to the membrane with a blue line.

Figure 1-2. Schematic depicting known Thorase functions.

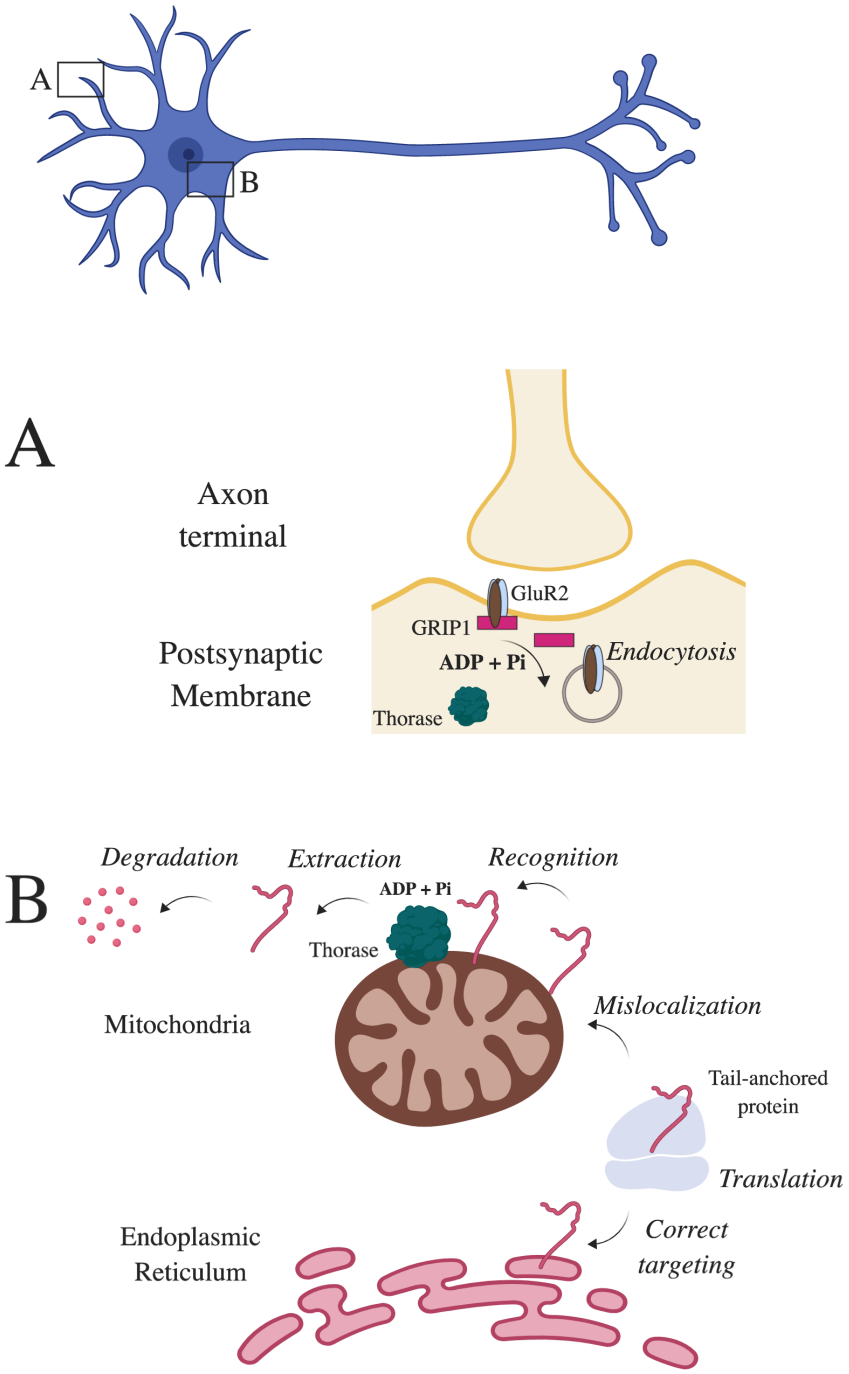

Figure 1-2. Schematic depicting known Thorase functions. A, in postsynaptic membranes, in an ATP-dependent manner, Thorase stimulates the endocytosis of GluA2 subunit-containing AMPA receptors by disrupting its interaction with GRIP1, thereby regulating neuronal excitability. **B,** in mitochondria, in an ATP-dependent manner, Thorase recognizes tail-anchored proteins that have been erroneously targeted to the outer mitochondrial membrane, and ensures organellar integrity by extracting them and promoting their degradation. This illustration was created using BioRender and adapted from Pignatelli et al (2017) and Hegde (2014).

Figure 1-3. Schematic summarizing mTORC1 regulation.

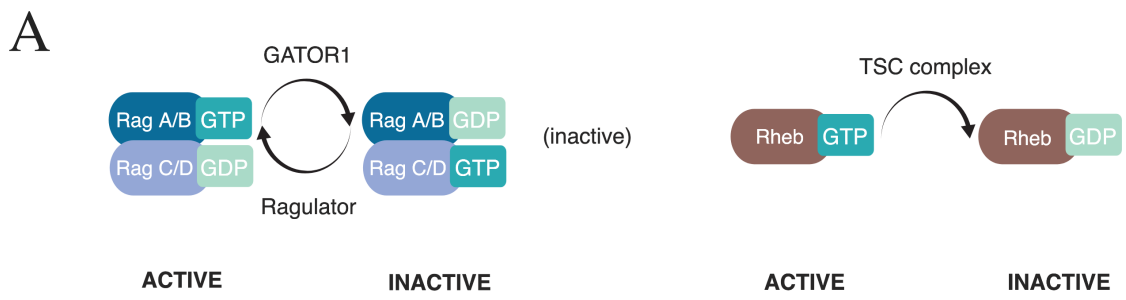

B

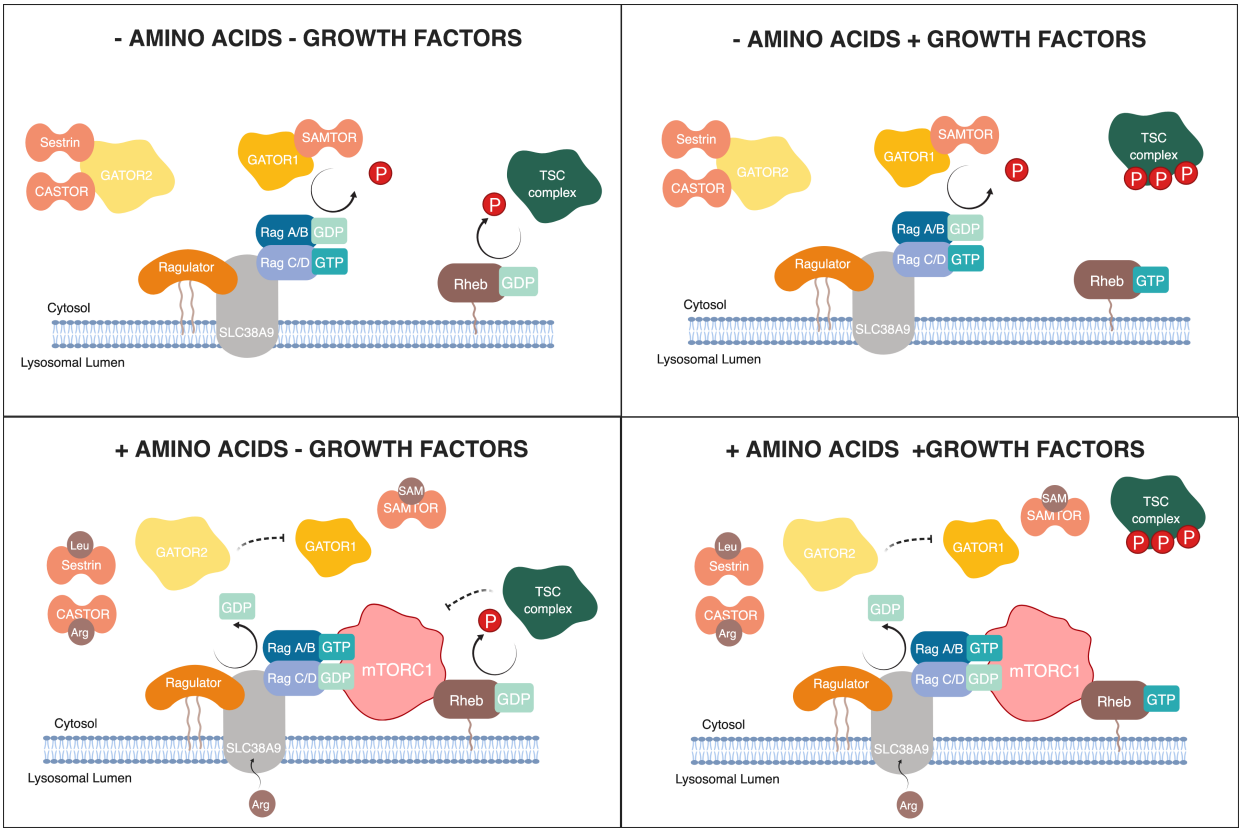

Figure 1-3. Schematic summarizing mTORC1 regulation. A, different small G proteins regulate the activation of mTORC1. RagA/B and RagC/Ds, and their activation depends on their nucleotide-binding status, with RagA/Bs active when bound to GTP, and RagC/Ds active when bound to GDP. GATOR1 stimulates the inactivation of Rag proteins, while Ragulator induces their activation. GTP-bound Rheb can directly activate mTORC1 activity, and the TSC complex prevents this with its GTPase Activating Protein (GAP) activity towards Rheb. **B,** Both amino acids and growth factors are required for full mTOR activation (AND-gate signaling). In the absence of amino acids and growth factors, GATOR1 and TSC complexes inhibit RagA/Bs and Rheb, respectively, by stimulating their GTPase activity. In the presence of growth factors alone, the TSC complex is phosphorylated and thus released from the lysosome. In the presence of amino acids alone, leucine-sensing Sestrin and arginine-sensing CASTOR impede the inhibitory effects of GATOR2 over GATOR1, and SAM-loaded SAMTOR no longer stimulates GATOR1 GAP activity, and therefore Rag proteins can recruit the mTORC1 to the surface of the lysosome. However, the concomitant presence of TSC complex at the lysosome inhibits mTORC1 activation through its inhibitory effects on Rheb. In the presence of both amino acids and growth factors, mTORC1 can be recruited to the lysosome and be directly activated by GTP-loaded Rheb. This illustration was created using BioRender and adapted from Valvezan & Manning (2019).

Chapter 2. Characterization of the effects on mitochondrial function of a novel homozygous ATAD1 mutation linked to a lethal encephalopathy in neonates

Introduction

ATAD1/Thorase was recently discovered as neuroprotective protein that belongs to the superfamily of AAA+ ATPases, involved in the unfolding of proteins and disassembly of protein complexes and aggregates, amongst other functions. In postsynaptic membranes, Thorase promotes the internalization of AMPA receptors by disrupting the interaction of AMPA receptor subunit, GluA2 and the AMPA receptor-binding protein, GRIP1 (Zhang et al, 2011). In mitochondria and peroxisomes, Thorase ensures the extraction of tail-anchored protein that are mislocalized, particularly upon cellular stress.

Recently, the first pathogenic human variant in Thorase linked to a congenital disease presenting with severe hypertonia, seizures, and death in a consanguineous family was reported (Ahrens-Nicklas et al, 2017). Supportive of its emerging importance in neurological disease, here we report a second pathogenic Thorase variant linked to a lethal encephalopathy affecting 3 newborn siblings in a consanguineous family. Exome-sequencing and subsequent variant analysis under an assumed recessive pattern of inheritance revealed a 2 base-pair deletion (c.1070_1071delAT), resulting in a frameshift at codon 357 and consequent translation of 14 novel codons at the C-terminal end of the protein (p.(His357Argfs*15).

In order to establish a relationship between genotype and phenotype for this new variant, we performed a series of biochemical assays to determine whether any of the known Thorase functions was affected and may therefore explain the severe clinical manifestations in the 3 siblings that ultimately led to their early death.

Results

Mutant Thorase is expressed in patient-derived fibroblasts

ATAD1 mRNA analysis from patient fibroblasts had suggested that, as a consequence of the frameshift, additional amino acid residues would be incorporated at the C-terminal end of the protein. To assess whether this altered C-terminal end of the protein would affect global protein stability, we examined the amount of ATAD1 protein in patient cells via immunoblotting. We observed no significant changes in the total levels of ATAD1 protein, suggesting that the altered protein product escaped cellular degradation (Figure 2-1).

The ATAD1 mutation p.(His357Argfs*15) leads to reduced amounts of some mitochondrial proteins in patient-derived fibroblasts

Previously, ATAD1 deletion in human cell lines was shown to cause an accumulation of peroxisomal biogenesis factor 26 (PEX26) and Golgi SNARE 28 kDa (GOS28) (Chen et al, 2014). In patient cells expressing C-terminal mutant Thorase, we found PEX26 protein levels were slightly lower compared to cells derived from healthy individuals. In addition, other mitochondrial proteins, including cytochrome c oxidase subunit 4 (COX4), hexokinase 1 (HXK1), and voltage-dependent anion channel 1 (VDAC1) were

also reduced (Figure 2-2). Thus, the frameshift mutation in ATAD1 seems to affect the stability or expression of peroxisomal and mitochondrial proteins.

Discussion

Combined with the results from other experiments, these data contributed to our recent report that pathogenic p.(His357Argfs*15) confers a gain-of-function to ATAD1, reportedly by locking the protein in an active oligomeric state without interfering with its ATP binding or hydrolyzing activity (Piard et al, 2018). Although the levels of several proteins were reduced compared to controls, mitochondrial morphology and respiratory capacity seemed unaltered. In contrast, cross-linking and imaging experiments with primary cortical cultures expressing the mutant form of Thorase ectopically showed reduced surface levels of AMPAR subunit GluA2, suggesting that mutant Thorase may induce excessive internalization of AMPA receptors.

Our previous report on a pathogenic mutation of Thorase (p.Glu276*) phenotypically resembled the loss-of-function in mouse models of Thorase deficiency. Surprisingly, there was extensive overlap clinically between the probands of both consanguineous families, including muscle stiffness since birth. This suggests that perhaps this C-terminally extended form of Thorase may act as dominant negative form for some but not all functions of the AAA+ ATPase.

Given the striking clinical parallelisms between a girl born to consanguineous parents in 1992 with congenital stiffness and the patients described in the reports by Ahrens-Nicklas

and Piard, Wolf and colleagues performed targeted Sanger sequencing of ATAD1 in muscle DNA isolated from the patient. This revealed a homozygous mutation at the last nucleotide of the second exon (c.162G > C), which was predicted to replace the highly conserved amino acid glutamine at position 54 to histidine (p.Gln54His) or to disrupt the splicing due to removal of the splice donor site of intron 2 (Wolf et al, 2018). Although this mutation would likely result in a loss of protein function, genotype-phenotype studies to validate this hypothesis would be necessary.

Given these three reports, ATAD1 is now established as a hyperekplexia (congenital stiffness) disease-causing gene.

Material and Methods

Maintenance of patient- and control-derived fibroblasts

Fibroblasts were maintained in Dulbecco's modified Eagle medium (DMEM, Corning Cellgro) plus 10% (v/v) fetal bovine serum (FBS) and 1% (v/v) Penicillin-Streptomycin (Corning Cellgro), at 37^{o}C with a 5% CO2 atmosphere in a humidified incubator.

Measurement of peroxisomal and mitochondrial protein expression

Thorase expression and comparative immunoblot analyses were performed using cell lysates from patient and control fibroblasts. Protein concentrations were determined by BCA protein assay (PierceTM, Thermo Scientific) and 20 mg were resolved on SDS-PAGE gels. Immunoblot membranes were stained with Ponceau solution to ensure equal loading of protein samples. Immunoblot analyses were performed using antibodies to

COX4, Hexokinase 1 (HXK1), PEX26, VDAC1 and actin (Sigma) as control for loading. Band intensities were quantified using ImageJ (NIH) and normalized to actin. The values obtained from ImageJ were further analyzed to determine significant differences using GraphPad Prism software (GraphPad).

Acknowledgements

This work was supported by a grant from the National Institute on Drug Abuse, P50DA000266.

This chapter is modified from:

Piard, J., Umanah, G.K.E., Harms, F.L., Abalde-Atristain, L., Amram, D., Chang, M., Chen, R., Alawi, M., Salpietro, V., Rees, M.I., Chung, S.K., Houlden, H., Verloes, A., Dawson, T.M., Dawson, V.L., Van Maldergem, L., Kutsche, K. (2018) A homozygous ATAD1 mutation impairs postsynaptic AMPA receptor trafficking and causes a lethal encephalopathy. Brain. 141(3):651-661. doi: 10.1093/brain/awx377.

Figure 2-1. Mutant Thorase is expressed in patient-derived fibroblasts.

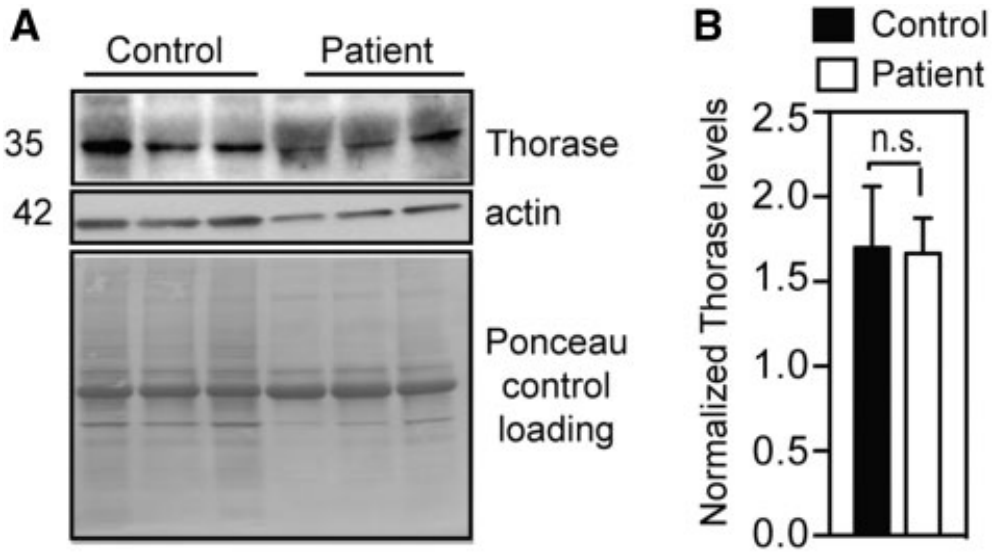

Figure 2-1. Mutant Thorase is expressed in patient-derived fibroblasts.

A, Immunoblot of lysates obtained from patient and control fibroblasts. Expression of Thorase was monitored using anti-Thorase antibody, and anti-actin antibody was used to control for equal loading. As the anti-Thorase antibody was generated against the C-terminus and this region contains a new amino acid composition in the mutant, detection of Thorase in patient cells was difficult (compare the clear band in control and the diffuse band in patient cells). **B,** Optical densitometry quantification of A. Values represent the mean +/- SEM (n = 3, n.s. $P > 0.05$, Tukey's multiple comparison tests).

Figure 2-2. The ATAD1 mutation p.(His357Argfs*15) leads to reduced amounts of some mitochondrial proteins in patient-derived fibroblasts.

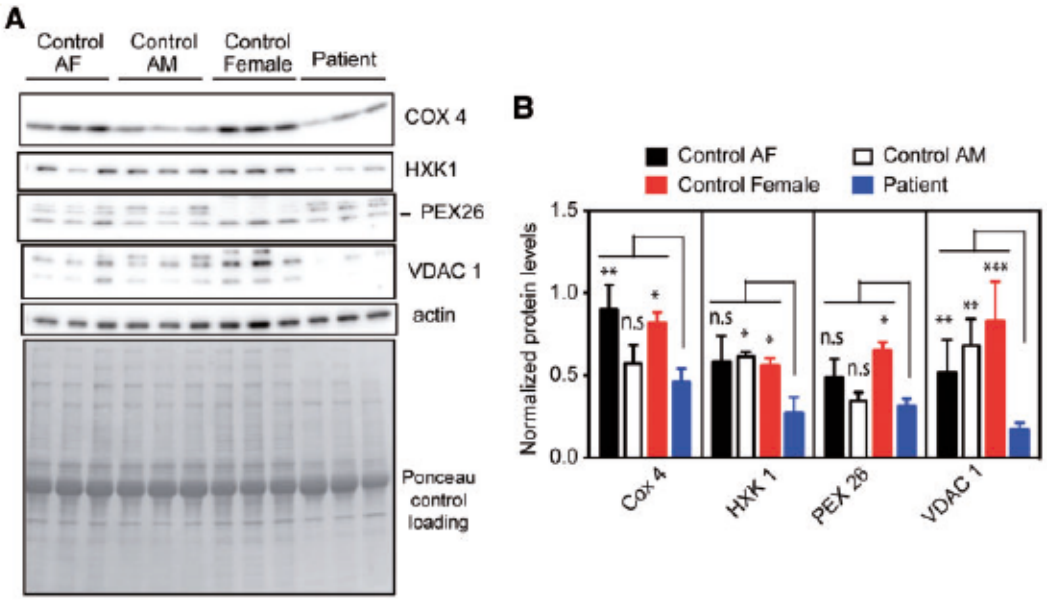

Figure 2-2. The ATAD1 mutation p.(His357Argfs*15) leads to reduced amounts of some mitochondrial proteins in patient-derived fibroblasts. A, Immunoblots of lysates obtained from patient and control fibroblasts. COX4 = cytochrome c oxidase subunit 4; HXK1, = hexokinase 1; PEX26 = peroxisomal biogenesis factor 26; VDAC1 = voltage dependent anion channel 1. **B,** Optical densitometry quantification of (A). Values represent the mean +/- SEM (n = 3, ***P < 0.01, **P < 0.05, *P < 0.10, n.s. > 0.10, two-way ANOVA, Tukey's multiple comparison tests).

Chapter 3. AAA+ ATPase Thorase Regulates mTOR Signaling Through the Disassembly of the mTOR Complex 1

Introduction

Thorase, also known as ATPase family AAA domain-containing protein 1 (ATAD1), belongs to the family of AAA+ ATPases associated with diverse cellular functions, which use energy garnered from ATP hydrolysis to disassemble protein complexes (Dai et al, 2010; Zhang et al, 2011). Thorase controls the endocytosis and internalization of α-amino-3-hydroxy-5-methyl-4-isoxazolepropionic acid receptors (AMPARs) through the disassembly of the AMPAR/glutamate receptor–interacting protein 1 (GRIP1) complex, thereby contributing to the regulation of synaptic plasticity, learning and memory (Zhang et al, 2011; Pignatelli et al, 2017; Umanah et al, 2017). Thorase also exerts an important function in maintaining mitochondrial and peroxisomal integrity by extracting mislocalized proteins out of these organelles (Chen et al, 2014; Okreglak et al, 2014; Prendergast et al, 2014). Recently, we have identified patients harboring Thorase mutations that suffer from a devastating neurological disease, with symptoms that include epilepsy in patients with loss-of-function mutations and aberrant or delayed myelination in patients with gain-of-function mutations (Umanah et al, 2017; Ahrens-Nicklas et al, 2017; Piard et al, 2018; Wolf et al, 2018).

Because Thorase abnormalities in humans show a broad clinical spectrum, and because Thorase belongs to a family of proteins known to perform multiple functions at a time,

we sought to discover novel roles for Thorase in the cell that could allow us to better understand its protective effects. For that, we decided to take an unbiased approach and search for novel Thorase interactors in the brain.

Results

Thorase interacts with mTOR kinase

In a search for additional novel Thorase-interacting proteins, we used recombinant GST-tagged Thorase to pull down potential Thorase interactors from whole brain lysates (Fig. 3-1A). Among the putative Thorase binding partners, mass spectrometry identified the mTOR kinase (Fig. 3-1B, Fig. 3-5A). When separating protein complexes pulled down by recombinant Thorase from brain lysates according to their molecular size using fast protein liquid chromatography (FPLC), we confirmed via immunoblotting that endogenous mTOR and recombinant Thorase co-exist in complexes of high molecular weight (FPLC fractions 1-4 in Fig. 3-1C, FPLC fractions 2-3 in Fig. 3-5B). Thorase preferentially binds to mTOR, rather than mTORC1-associated proteins Raptor, S6K or 4EBP1 (Fig. 3-5, C and D). Binding between Thorase and mTOR is direct, as revealed by our experiments performed *in vitro*, where purified recombinant mTOR and Thorase proteins alone assembled into high molecular weight complexes similar to those observed *in vivo* (Fig. 3-5E). Binding of Thorase and mTOR is strong in the presence of a non-hydrolizable ATP analog (ATPgammaS), which generally enhances binding of Thorase to its substrates (Zhang et al, 2011; Umanah et al, 2017), both when we pull down endogenous Thorase (Fig. 3-5, C and D) or in the reverse pull down of endogenous mTOR (Fig. 3-1, D and E). Concomitant to a strong binding between Thorase to mTOR,

we detected a decrease in mTOR binding to the mTORC1 component Raptor, and mTORC1 substrates S6K and 4EBP1 (Fig. 3-1 D-F). In contrast, when we performed immunoprecipitation assays in the presence of hydrolizable ATP or ADP, both pull down of mTOR by Thorase and pull down of Thorase by mTOR was less efficient, as was the case with other Thorase interactors (Zhang et al, 2011; Umanah et al, 2017) (Fig. 3-1 D and E, Fig. 3-5 C and D). A weaker interaction between Thorase and mTOR in the presence of ADP or hydrolizable ATP correlated to an enhanced binding of mTOR to Raptor, 4EBP and S6 (Fig. 3-1 D-F). Moreover, in the absence of Thorase, Raptor, S6K and 4EBP1 proteins co-immunoprecipitated with mTOR regardless of what nucleotide we added to the reaction (Fig. 3-1, D-F). Overall, these results suggest that Thorase directly interacts with mTOR and that it may be involved in the disassembly of the mTORC1.

Thorase disassembles the mTOR complex 1

To further elucidate the molecular interaction between Thorase and the mTORC1, we used single-molecule pull-down (SiMPull), which combines traditional immunoprecipitation with single molecule fluorescence imaging, allowing for the study of the binding dynamics within protein complexes (Aggarwal and Ha, 2013; Jain et al, 2011; Jain et al 2014). We pulled down mTORC1 on slides from cell extracts by capturing the mTORC1-specific protein Raptor tagged with red fluorescent protein (RFP), and imaged yellow fluorescent protein (YFP)-tagged mTOR and RFP-Raptor (Fig. 3-2A, Fig. 3-6A). The addition of recombinant Thorase led to a decrease in the number of mTOR molecules on the slide in a dose-dependent manner and with a mid-

point Thorase concentration of 0.33 nM, consistent with a high avidity binding of Thorase to mTOR, resulting in its dissociation from Raptor and other mTORC1 components (Fig. 3-2 B and C, Fig. 3-6 C and D). There was no significant change in the number of RFP-Raptor spots after the addition of Thorase (Fig. 3-2B, Fig. 3-6 C and D), and Thorase did not disassemble the PKA complex that was used as a control (Jain et al, 2011) (Figs. 3-6, B, E and F). When we pulled down mTORC1 on slides via the capture of YFP-mTOR and added Cy5-labeled Thorase (Fig. 3-6G), the number of RFP-Raptor spots decreased while the number of Cy5-Thorase spots increased, suggesting that Thorase displaces Raptor and binds to mTOR (Fig. 3-6, H and upper panels on I). When pulling down mTORC1 via capture of Raptor or in the control experiments with the PKA complex, a significantly smaller number of Cy5-Thorase molecules were detected bound to Raptor or the PKA complex, respectively (Fig. 3-6, lower panels on I and J), supportive of the specificity of binding of Thorase to mTOR. mTOR disassembly from Raptor by Thorase is dependent on ATP binding, as addition of Thorase in the presence of the non-hydrolyzable ATP analog AMP-PNP promoted a significantly sharper decrease of YFP-mTOR and RFP-Raptor spots, compared to Thorase addition in the presence of ADP or ATP (Fig. 3-7, A-F). Similarly, the efficiency of disassembly of mTOR, as measured by disappearance of YFP-mTOR spots, decreased in the presence of Thorase mutants Walker A and Walker AB that are incapable of binding ATP, as compared to wild type Thorase or mutant Walker B which can bind ATP but not hydrolyze it (Zhang et al, 2011) (Fig. 3-7, G and H). In the absence of Thorase, the dimer forms of mTOR and Raptor were the dominant species (Aggarwal and Ha, 2013; Jain et al, 2011; Jain et al 2014), whereas monomeric mTOR and Raptor emerged as the

dominant species following Thorase addition (Fig. 3-7, C, F and I). Detailed stoichiometric analyses of the mTORC1 further confirms that the dimeric species, mT_2R_2, dominates in the absence of Thorase, whereas the monomeric species, mT_1R_1, dominates in the presence of Thorase (Fig. 3-2 D-E, Fig. 3-7J). This suggests that Thorase disassembles the mTORC1 by removing mTOR molecules one at a time (Fig. 3-2 D-E, Fig. 3-7 C, F, I and J). To determine the binding site of mTOR in Thorase, we generated N-terminal (N40, N50, N60, N70, N90, N100) and C-terminal (C10 and C20) truncated variants (Fig. 3-8A). GST-Thorase and mTOR pulldown analyses suggest that deletion of the residues 70-90 inhibits the binding of mTOR to Thorase (Fig. 3-8, B-E). SiMPull analyses confirm that the N-terminus of Thorase is critical for binding to mTOR, since mutants lacking the first hundred amino acid residues of Thorase disassemble the mTOR-Raptor complex less efficiently (Fig. 3-8, F-G). Collectively, these findings show that Thorase binds strongly to mTOR to mediate the disassembly of the mTORC1.

Lack of Thorase results in excessive mTORC1 activity *in vitro* and *in vivo*

To verify that mTOR is a substrate of Thorase *in vivo*, we analyzed the status of the mTOR signaling pathway in the brains of mice lacking Thorase. The total and phosphorylated levels of several mTORC1-related proteins were increased in the cortices and hippocampi of Thorase knockout mice, suggesting that elevated mTORC1 signaling occurs in the absence of Thorase (Fig. 3-3 A-C, Fig. 3-9 A and B). Consistent with upregulated mTORC1 signaling, we found an increased abundance of poly-ubiquitinated proteins in the brains of Thorase knockout mice (Fig. 3-3, D and E). We confirmed the same mTORC1 hyperactivity occurs in fibroblasts derived from Thorase knockout mouse

embryos, which presented increased levels of mTORC1 signaling (Fig. 3-9, C and D) and consequent increased amounts of newly-synthesized proteins (Fig. 3-9, E and F).

Next, we sought to determine whether the absence of Thorase and subsequent dysregulation of mTORC1 disassembly may have any physiological consequences. mTORC1 activity is central to regulating oligodendrocyte differentiation and myelination (Zou et al, 2011). We found that the levels of myelin and oligodendrocyte markers CNP, MBP, TMEM10 and MOG were higher in both the cortices and hippocampi of mice lacking Thorase (Fig. 3-4, A and B). We could also detect higher levels of myelin through black gold staining in the brains of Thorase knockout mice, as well as increased levels of MBP and TMEM10 in axon fibers (Fig. 3-4, C and E) which also appeared more compact (Fig. 3-10A). The numbers of mature oligodendrocytes, which can be identified by double staining with Olig2 and CC1, were higher in the absence of Thorase, and this may account for the increased levels of myelin observed (Fig. 3-4 D and E, Fig. 3-10B). Accordingly, the myelin sheath of axons in the optic nerve appeared significantly thicker under transmission electron microscopy in the absence of Thorase (Fig. 3-4F, Figs. 3-10 C-F) and, consequently, the g ratio (or ratio of the inner diameter to the total outer diameter of myelinated axons) was smaller in the optic nerves of Thorase knockout mice (Fig. 3-4G). Furthermore, Thorase knockout mice present a non-significant increase in the number of myelinated axons (Fig. 3-4H). These results support the idea that the absence of Thorase results in sustained mTORC1 activity, with subsequent alteration of the physiological processes downstream of mTORC1 signaling, including increased myelination in the optic nerve.

Rapamycin can alleviate the mTORC1 hyperactivity observed in the absence of Thorase

Lastly, we tested whether the mTOR inhibitor, rapamycin, could alleviate the mTORC1 hyperactivity observed when Thorase is lacking. Indeed, the levels of phosphorylated S6 in fibroblasts derived from either Thorase knockout mice or wild type littermates decreased significantly after the treatment with rapamycin as compared to vehicle-treated counterparts, with phosphorylated S6 levels equally as low in rapamycin-treated wildtype and Thorase knockout fibroblasts (Fig. 3-4, I and J). In contrast, the levels of the rapamycin-resistant T37/46 site in 4EBP did not significantly change in either wildtype or Thorase knockout fibroblasts treated with rapamycin (Fig. 3-4, I and J). Consequent to the rapamycin treatment, the synthesis of new proteins in these fibroblasts as measured by incorporation of radiolabeled methionine was decreased as well (Fig. 3-4, K and L). Thorase knockout mice have a very short lifespan, with most mice dying three weeks after birth, due to epileptic seizures (Zhang et al, 2011). To test whether mTORC1 hyperactivity may be accountable for the pathology underlying the sudden death of Thorase knockout mice, we treated mice with rapamycin. Decreasing mTOR activity with rapamycin lengthened the lifespan of mice lacking Thorase, with a significant increase in their median survival compared to vehicle-treated Thorase knockout mice (Fig. 3-4M). Some mice doubled their life span, surviving for over 60 days postnatally, compared to vehicle-treated knockout littermates (Fig. 3-4M). These results taken together indicate that, in mice lacking Thorase, mTOR activity is increased and this accounts, in part, for the phenotype of Thorase knockout mice.

Discussion

In summary, we have found that AAA+ ATPase Thorase serves as a molecular motor that disassembles the mTORC1, which is central to attenuating its downstream signaling activity. By directly binding to mTOR, Thorase prevents its binding to other mTORC1 components. In the absence of Thorase, mTORC1 signaling is hyperactive, leading to the dysregulation of several processes downstream of mTORC1 signaling, such as *de novo* protein synthesis at a cellular level, or myelination of axons in the brain physiologically. The regulation of mTORC1 activity by Thorase may also be relevant to human disease, as we have identified patients harboring Thorase mutations that suffer from a devastating neurological disease, with symptoms that include epilepsy in patients with loss-of-function mutations and aberrant or delayed myelination in patients with gain-of-function mutations. Deregulation of the mTOR signaling pathway underpins numerous human diseases, including epilepsy (Crino, 2015). Overall, our discovery that Thorase is a novel modulator of mTOR activity that acts through the disassembly of the mTORC1 sheds some light onto how the pathway is terminated and provides a potential new therapeutic avenue to treat the myriad of human diseases related to dysregulated mTOR signaling.

Material and Methods

Antibodies and chemicals

We purchased anti-Thorase (NeuroMab Cat# 75-157 RRID:AB_2290002) from UC Davis/NIH NeuroMab facility. Primary antibodies for mTOR (#2983), phos-S2448 mTOR (#5536), phos- S2481 mTOR (#2974), Raptor (#2280), phos-S792 Raptor (#2083), anti-Rictor (#2114), phos- T1135 Rictor (#3806), p70 S6K (#2708), phos-T389

p70 S6K- (#9205), anti-S6 (#2217), phos- S240/244 S6 (#2215), 4EBP1 (#9644), phos-T37/46 4EBP1 (#2855), elF4B (#3592), phos-S422 elF4B (#3591), ULK1 (#8054), phos-S757 ULK1 (#6888), Rheb1 (#13879) were purchased from Cell Signaling Technologies. Antibodies for Tomm20 (#ab186735), anti-rabbit (#ab98467) and anti-mouse (#ab6823) were purchased from Abcam. Anti-rabbit Alexa Fluor®647 Conjugate (#A32733), anti-mouse Alexa Fluor®594 Conjugate (#A11032) and Anti-rabbit Alexa Fluor®488 Conjugate (#A32731) secondary antibodies were purchased from Invitrogen. Anti-CC1 and anti- MBP antibodies were purchased from Calbiochem (San Diego, CA); anti-Olig2 antibody from Millipore (Billerica, MA). Tmem10 antibody was generated by immunizing New Zealand white rabbits with bacterial His-tagged fusion protein. Black Gold II Myelin Staining Kit was purchased from Millipore. All antibodies used for SiMPull were obtained from commercial sources as follows: biotinylated anti-RFP from Abcam (ab34771) and anti-YFP from Rockland Antibodies and Assays. DAPI was purchased from Invitrogen (Molecular Probes). Hank's balanced salt solution (HBSS) (#14025), Neurobasal (#21103049), Dulbecco's Modified Eagle Medium (DMEM) (#11995), Fetal Bovine Serum (FBS) (#16140071), and B-27 supplement (#17504044) were purchased from Gibco. L-Glutamine (#25-005-CI) and Penicillin-Streptomycin (#30-002-CI) were purchased from Corning. Poly-L-ornithine hydrobromide (#P3655-1G) was purchased from Sigma Aldrich.

Other reagents include Prescission Protease (#27-0843-01 GE Healthcare), ATPgammaS, Adenosine 5'- (3-thiotriphosphate) tetralithium salt (A1388-25MG MilliporeSigma) Nickel-NTA (Qiagen), glutathione beads (#SKU 16101 Pierce), QuickChange site-

directed mutagenesis kit (Stratagene, USA), E. coli BL21(DE3) RIL cells (E. coli BL21(DE3) RIL cells (#69450 Novagen), Neutravidin (#31000 Thermo Fisher) and BSA (#B9000S New England Biolabs).

Plasmids

Thorase was cloned into lenti-viral plasmid pLVX-IRES-mCherry (Thorase, Ires Mcherry), the AAV-viral plasmid pAM/CBA-pl-WPRE-BGH, with FLAG epitope tag (Thorase-FLAG) and lenti-viral cFUGW plasmid (Thorase-GFP) vectors. Thorase coding sequence was inserted into pLVX-IRES-mCherry (Clontech, USA) or pAM/CBA-pl-WPRE-BGH between XhoI and BamHI and into cFUGW vector between BamHI and AgeI sites. These plasmids were used for Thorase expression in HEK293 cells, mouse embryonic fibroblasts (MEFs), or primary neurons. Thorase was also cloned into pGEX6P-1 (Addgene) and pET32a (Novagen) vectors (BamHI and XhoI sites) and were expressed as GST and His6 fusion recombinant proteins, respectively. Site directed PCR and restriction enzyme digest were performed to generate Thorase truncated variants, N30, N40, N50, N60, N70, N90, N100 which have the first 30, 40, 50, 60, 70, 90 and 100 residues deleted, respectively. Thorase deletion variants, C10 and C20 with the last 10 and 20 residues deleted, respectively, were also generated. GST-tagged mTOR was generated by inserting the full-length coding sequence at the NotI site in pGEX6P-1. All plasmids constructs were verified by sequencing at The Johns Hopkins University DNA sequencing facility. Lamp1-RFP plasmid was commercially obtained from Addgene (Plasmid #1817). All plasmids used for SiMPull were obtained from commercial sources

as follows: peYFP-C1-mTOR (Addgene Plasmid #73384) and pRK5-HA-mCherry-Raptor (Addgene Plasmid #73386).

Lentivirus Generation

Lentiviruses expressing Thorase were generated by the transient transfection of HEK293T cells with lentiviral plasmids described above using FuGENE HD Transfection Reagent (Roche Applied Science). The cells were co-transfected with the Thorase lentiviral plasmids, the transcomplementation plasmids (pLP1 and pLP2), and the plasmid encoding the vesicular stomatitis virus envelope glycoprotein (VSVG) followed by sodium butyrate treatment 6 hours after transfection. The medium was replaced 24 hours after transfection. Viral particles were harvested by collecting medium 48 hours and 72 hours after transfection and centrifuged at 3000g for 10 minutes, then filtered through a 0.45 um membrane. Viral particles were then concentrated by ultracentrifugation (2 hours, 25,000 rpm, rotor SW28). The viruses were stored at -80^{o}C until needed. The expression of Thorase was verified by infecting HEK293 cells with viruses and cells examined under fluorescence microscope 24-48 hours after infection. Cells were harvested and lysates were resolved on SDS-PAGE and immunoblotted by probing with anti-Thorase.

Recombinant protein purification

GST- tagged fusion proteins were expressed in Escherichia coli strain BL21-CodonPlus (DE3)- RIPL (Stratagene, Agilent Tech. Div., USA) bacteria. Small cultures (100 ml) were grown overnight at 37^{o}C and then transferred to 2 liter cultures for another 8 hours.

Cells were cold shocked at 4°C for 1 hour before adding 1mM IPTG for overnight induction at 16°C. Cells were lysed using micro-Fluidizer in binding buffer (1x phosphate buffer, pH 7.5, 150 mM NaCl, 2.5 mM MgCl2, 1 mM DTT, 5% glycerol) containing protease inhibitors and purified by using GST beads (GE Healthcare) following the manufacturer's instructions. To obtain untagged purified proteins, GST-tagged proteins bound to the GST beads were treated with Prescission protease (GE Healthcare) to remove the GST tags. Samples were further purified using ion 5 exchange chromatography and/or size-exclusion chromatography. Purity of the recombinant proteins was assessed by SDS-PAGE followed by Coomassie blue staining and immunoblotting.

Pull down assays

For the identification of Thorase binding partners, recombinant GST-Thorase purified on beads was mixed with mouse whole brain lysates in the presence of non-hydrolysable ATP (ATPgammaS) in buffer A (50 mM HEPES, pH 7.5, 150 mM NaCl, 2.5 mM MgCl2, 1 mM DTT, 5% glycerol) and incubated with end-over-end mixing for 2 hours. The beads were then extensively washed with buffer A containing ATPgammaS, and Thorase was cleaved from the GST beads with PreScission protease (GE Healthcare). The supernatant containing different protein complexes bound to Thorase was loaded into size-exclusion chromatography to separate the complexes. The different fractions eluted from the column were resolved by SDS-PAGE and individual bands (proteins) were excised for mass spectrometry analyses. Immunoblotting was used to confirm the presence of proteins identified by mass spectrometry.

Co-immunoprecipitation of endogenous Thorase and mTOR was carried out using lysates of whole mouse brains. Freshly isolated whole brains from wildtype or Thorase knockout mice were powderized under dry ice and homogenized in buffer A containing protease inhibitors with or without 2 mM ADP, ATP or ATPgammaS. Triton X-100 was added to a final concentration of 1% followed by rotation for 2 hours at 4^{o}C. Extracts were centrifuged at 15,000g for 30 minutes and supernatant was incubated for 3 hours at 4^{o}C with Protein G beads (Pierce) pre-bound with anti- Thorase or anti-mTOR antibodies. The beads were washed 3 times with buffer A plus 1 mM ADP, ATP or ATPgammaS and bound proteins were eluted from beads using 1x SDS-PAGE Laemmli buffer (Sigma) with DTT. The eluted proteins were resolved by SDS-PAGE. Immunoblotting analyzes were carried out with antibodies to Thorase, mTOR, Raptor, S6K and 4EBP1.

For in vitro pull down of Thorase and mTOR, recombinant GST-Thorase (wildtype or variants) or GST-mTOR purified on beads were mixed with mouse whole brain lysates in the presence of 2 mM ADP, ATP or ATPgammaS in buffer A and incubated with mixing for 2 hours. The beads were then extensively washed with buffer A containing 1 mM ADP, ATP or ATPgammaS. The beads were resuspended in 1 x SDS-PAGE sample buffer and eluted samples resolved by SDS-PAGE. Immunoblotting was used to confirm the presence of proteins bound to GST-tagged proteins. For assessing direct interaction between Thorase and mTOR, recombinant GST-Thorase purified on beads was mixed with purified non-tagged mTOR recombinant protein in the presence of 2 mM ATPgammaS in buffer A and incubated with mixing for 2 hours. The beads were then

extensively washed with buffer A containing 1 mM ATPgammaS. The sample eluted from the beads was loaded into sizeexclusion chromatography to separate the complexes. The different fractions eluted from the column were resolved by SDS-PAGE to confirm the presence of GST-Thorase and mTOR. Mass spectrometry was conducted at Harvard Medical School Taplin Spectrometry Facility.

Cell Culture

HEK293 and MEFs were maintained in at 37ºC with a 5% CO2 atmosphere in a humidified incubator, and grown in DMEM supplemented with 10% FBS and 1% PS. Transfections in HEK293 were performed with Lipofectamine 2000 Reagent (Invitrogen) according to the manufacturer's instructions.

Primary cortical neuron cultures were prepared from embryonic day 15 (E15) mouse pups and grown in Neurobasal media (Gibco) with B27 supplement (Gibco), 1% L-glutamine and 1% PS (complete neurobasal media), and maintained in at 37ºC with a 7% CO_2 atmosphere in a humidified incubator.

De novo protein synthesis assessment

Fibroblasts derived from wildtype or Thorase knockout mouse embryos were grown in 12 well plates (Falcon) to around 80% confluency, and pre-treated with vehicle DMSO or 500 nM rapamycin (LC laboratories) if needed. 25 uCi of 35S-L-methionine/35S-L-cysteine (PerkinElmer) per well were added to the media, and cells were incubated at 37ºC and 5% CO_2 for 1 hour. Cells were then washed twice with cold PBS, and lysed in

extraction buffer (2% NP-40, 50 mM Tris HCl, 150 mM NaCl, 5 mM EGTA, protease inhibitor cocktail), spun down and supernatants collected. Protein was concentrated with methanol/heparin, and protein pellets then resuspended in 8M Urea/150 mM Tris (pH 8.5). Samples were then analyzed in a LS 6500 Multi-purpose 9 Scintillation Counter (Beckman Coulter), and radioactive counts normalized to sample protein concentration as measured by Pierce BCA protein assay (Thermo Scientific).

Myelination studies

For immunohistochemistry experiments, mouse brains were prepared by cardiac perfusion and stained as described above. Black Gold staining (Millipore) was performed following the manufacturer's instructions. For optic nerve myelination analysis through electron microscopy, animals were perfused with 2% glutaraldehyde 2% paraformaldehyde (freshly prepared from EM-grade prill) 75 mM sodium cacodylate 75 mM phosphate (Sorenson's) 3 mM MgCl2, pH 7.2 at 1006 mOmols. After perfusion, animals were kept at 4^{o}C for two hours, then brains and optic nerves were carefully removed and placed in fresh fixative overnight at 4^{o}C. The following steps were kept cold (4^{o}C) until the 70% ethanol step, then run at room temperature. Samples were rinsed in 75 mM cacodylate 75 mM phosphate 3.5% sucrose MgCl2, pH 7.2 at 442 mOsmols for 45 min. Following buffer rinses, samples were post-fixed in 2% osmium tetroxide reduced with 1.6% potassium ferrocyanide, in the same buffer without sucrose for 2 hours on ice in the dark. Optic nerves were then rinsed in 100 mM maleate buffer with 3.5% sucrose pH 6.2, then en-bloc stained for 1 hour with filtered 2% uranyl acetate in maleate sucrose buffer, pH 6.2. Following en-bloc staining samples were dehydrated

through a graded series of ethanol to 100%, transferred through propylene oxide, embedded in Eponate 12 (Pella) and cured at 60 ^{o}C for two days. Sections were cut on a Riechert Ultracut E microtome with a Diatome Diamond knife (45 degree). 60nm sections were picked up on formvar coated 1 x 2 mm copper slot grids and stained with methanolic uranyl acetate followed by lead citrate. Grids were viewed on a Hitachi 7600 TEM operating at 80 kV and digital images captured with an XR50 5 megapixel CCD by AMT.

SiMPull experiments

HEK293 cells were transiently co-transfected with YFP-mTOR and mCherry-Raptor followed by cell lysis in lysis buffer (40 mM Hepes, pH 7.5, 120 mM NaCl, 10 mM sodium pyrophosphate, 10 mM b-glycerophosphate, 1X protease inhibitor mixture and 0.3% CHAPS). YFP-mTOR- and mCherry-Raptor-only lysates were obtained by transiently transfecting cells with YFP-mTOR and mCherry-Raptor, respectively. Lysates were centrifuged at 12,000 X g for 12 min at 4^{o}C and diluted 150-fold to obtain a surface density optimal for single-molecule analysis (~800 molecules in 5,000 μm2 imaging area). For control experiments, HEK293 cells were transiently transfected with PKA isoforms PKA-RIIb-Flag-mCherry and PKA-Ca-HA-YFP. After 24 hours of expression, cells were lysed using a buffer containing 10mM Tris pH 7.5, 1% NP-40, 150 mM NaCl, 1 mM EDTA, 1 mM benzamidine, 10 μg/ml leupeptin, 1mM NaF, 1mM Na3VO4. The lysate thus obtained was centrifuged at 14,000 X g for 20 minutes and subsequently used for SiMPull.

Recombinant Thorase was incubated with 20-fold molar excess of Cy5-maleimide dye (GE Healthcare Life Sciences) in 1X PBS buffer (Thermo Fisher Scientific) at room temperature for an hour and at 4^{o}C overnight. Unreacted dyes were removed by gel filtration using Zeba spin desalting columns (7K MWCO, Thermo Fisher Scientific). Single-molecule experiments were performed on a prism-type TIRF microscope equipped with an electron-multiplying CCD camera (EM-CCD). For single-molecule pull-down experiments, quartz slides and glass cover slips were passivated with 5000 MW methoxy poly-(ethylene glycol) (mPEG, Laysan Bio) doped with 2-5% 5000 MW biotinylated PEG (Laysan Bio). Cell lysates were pulled down with biotinylated antibodies against YFP or RFP, already immobilized on the surface via neutravidin-biotin linkage. Thorase interactions with mTORC1 and its individual components were studied by incubation of pulled-down mTORC1 or its individual components with a pre-determined concentration of Cy5-Thorase in T200-BSA buffer supplemented with 5 mM AMP-PNP (or ATP, Sigma-Aldrich), 20 mM MgCl2 and 10% Glycerol. 15 frames were recorded from each of 20 different imaging areas (5,000 μm2) and isolated single-molecule peaks were identified by fitting a Gaussian profile to the average intensity from the first ten frames. Mean spot-count per image for YFP and mCherry was obtained by averaging 20 imaging areas using MATLAB scripts.

Co-localization data were acquired from two or three separate movies from the same region of a slide using YFP, m-Cherry and Cy5 excitation. The co-localization criterion was set to a diffraction limited region of ~300 nm, which corresponds to 2 pixels for this TIRF setup. % co-localization was calculated as the % molecules co-aligned with the

pulled down component, unless otherwise stated. YFP, mCherry and Cy5 images taken from different areas were also overlapped to determine the probability of false co-localization arising from random spatial overlap of single molecules. Average % co-localization was calculated based on a minimum of 30 individual slide areas.

For photobleaching analysis, single-molecule fluorescent time traces from individual YFP or mCherry spots were manually scored for the number of photobleaching steps and the stoichiometry of the molecules was assessed subsequently as described before.

Animals

Thorase homozygous knockout mice and wildtype littermates were obtained by crossing heterozygous Thorase mice. Animal experiments were performed in compliance with the regulations of the Animal Ethical Committee of the Johns Hopkins University Animal Care and Use Committee.

Rapamycin treatment in mice

Wildtype or Thorase knockout mice were injected intraperitoneally with 6mk/kg Rapamycin (#R- 5000, LC laboratories) or vehicle (10% PEG400, 10% Tween 80 in water), 3 times per week starting at 10-14 days postnatally.

Study design and reproducibility

All biochemical and imaging experiments were repeated independently at least three times. For biochemical experiments involving brain tissue or mouse embryonic

fibroblasts, 3 biological replicates per group were used per experiment. For mouse survival experiments and immunohistochemical analysis, enough sample size (as determined via post hoc power analysis) was used, and mice pertaining to different litters were used. For biochemical experiments where 2 treatments were applied, 2 technical replicates per biological sample (3 biological replicates total per group) were used. We found our results reproducible when experiments were performed by 2 independent researchers. For mouse experiments where either vehicle or rapamycin was injected, an independent researcher randomly allocated mice to either treatment group. Regarding blinding during data collection, for immunofluorescence, immunohistochemistry and electron microscopy imaging, researchers were blinded to genotypes. For mouse survival analysis, researchers were blinded to both genotype and treatment groups.

Data analysis and statistics

All experiments were repeated at least three times and quantitative data are presented as the mean ± standard error of the mean (SEM) by GraphPad prism6 software (Instat, GraphPad Software). Statistical significance was assessed by ANOVA. The significant differences were identified by post-hoc analysis using the Tukey-Kramer post-hoc method for multiple comparisons. Assessments were considered significant with a $p < 0.05$ and non-significant with a $p > 0.05$. To assess the sufficiency of sample size, post hoc power analysis was performed, considering a power greater than 0.9 sufficient. Power analysis and sample size calculation for all experiments were determined using G*Power 3.1 software. Power was calculated as $1-\beta$, assuming $\alpha = 0.05$.

Acknowledgements

This work was supported by grants from the NIH/NIDA DA000266, DA044123 to T.M.D. and V.L.D and NIH/NINDS NS099362 to GKEU, NIH/NIGMS GM112659 to T.H., National Science Foundation Grant PHY-1430124 to T.H., and a La Caixa Foundation grant to L.A-A. T.M.D. is the Leonard and Madlyn Abramson Professor in Neurodegenerative Diseases and T.H. is an Investigator with the Howard Hughes Medical Institute.

This chapter was modified from:

A manuscript in preparation for submission: Umanah, G.K.E.*, Abalde-Atristain, L.*, Mitra, J., Yu, Z., Chang, M., Tangella, K., Chen, R., Delannoy, M., Aggarwal, V., Xiao, B., Worley, P., Ha, T., Dawson, T.M., Dawson, V.L. AAA+ ATPase Thorase Regulates mTOR Signaling Through the Disassembly of the mTOR Complex 1

*authors contributed equally to this work

Figure 3-1. Thorase interaction with mTOR is concomitant to a decrease in binding of mTOR to other mTOR complex 1-related proteins.

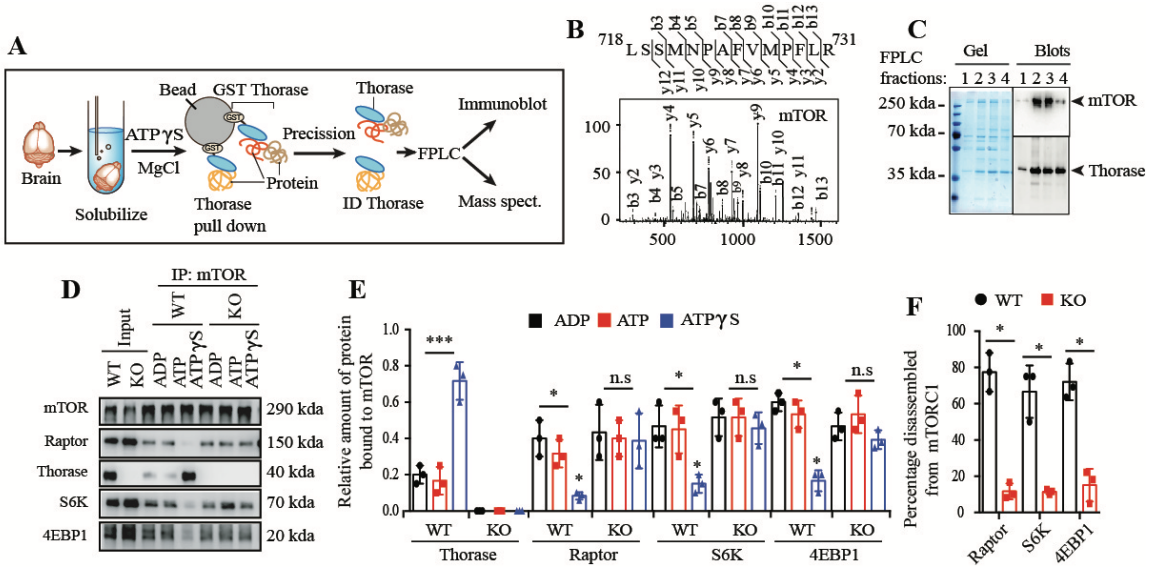

Figure 3-1. Thorase interaction with mTOR is concomitant to a decrease in binding of mTOR to other mTOR complex 1-related proteins. A, Schematic diagram of recombinant Thorase pulldown from brain lysates to identify novel binding partners through mass spectrometry. **B**, Representative mTOR peptide fragmentation detected by mass spectrometry after Thorase pulldowns. **C**, SDS-PAGE and immunoblots of FPLC fractions of Thorase pulldown of mTOR. **D**, Immunoblot images of mTOR pulldown from wildtype (WT) or Thorase knockout (KO) brain lysates in the presence of different nucleotides. **E**, Quantification of blots in D (n = 3). **F**, Graphical representation of percent disassembly of mTORC1-related proteins in D (n = 3). Data in E and F are mean ± standard error of the mean [SEM] of three independent experiments, ***$p < 0.001$, *$p < 0.05$, n.s $p > 0.05$, ANOVA with Tukey-Kramer post-hoc test compared with WT or control.

Figure 3-2. Thorase disassembles the mTOR complex 1.

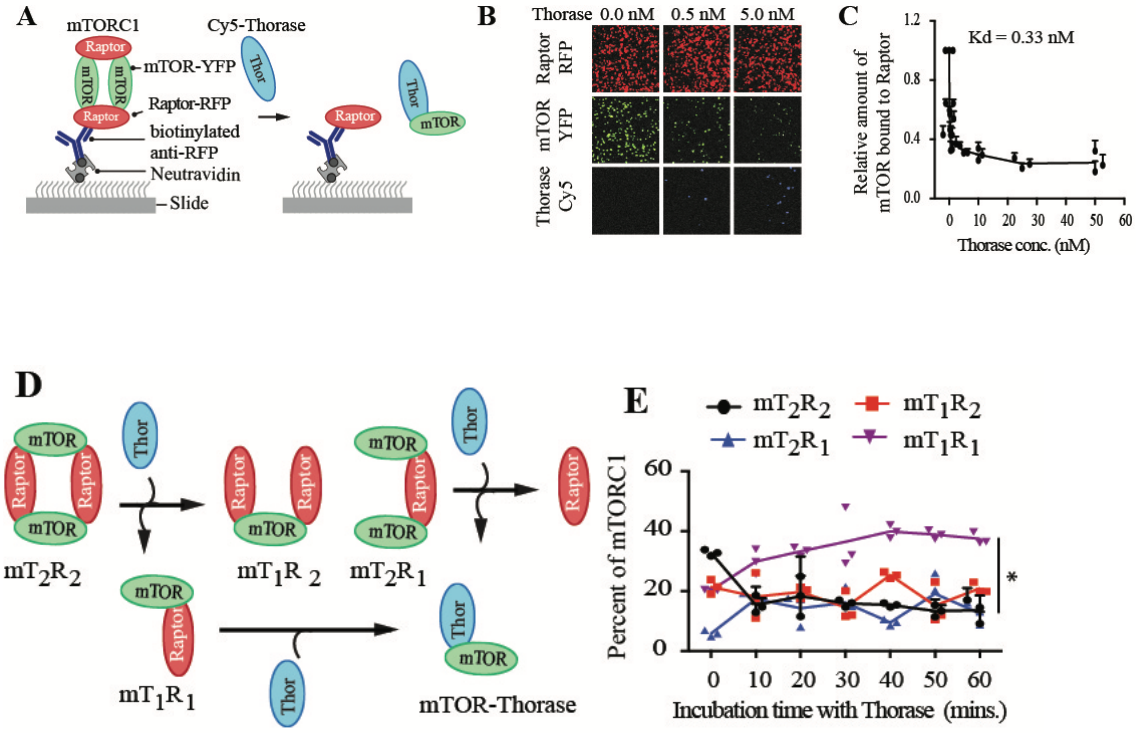

Figure 3-2. Thorase disassembles the mTOR complex 1. A, Schematic depiction of mTORC1 SiMPull in the presence of Thorase. **B**, Representative images from SiMPull shown in A with different concentrations of Thorase. **C**, Graphical representation of the kinetics of Thorase disassembly of mTOR-Raptor complex with a Kd value of 0.33 nM. **D**, Schematic diagram of SiMPull showing how Thorase disassembles mTOR-Raptor complex. **E**, Graphical representation showing the distribution of the different mTOR-Raptor species over time in the presence of Thorase (n = 3).

Figure 3-3. Thorase regulates the activity levels of the mTORC1 pathway.

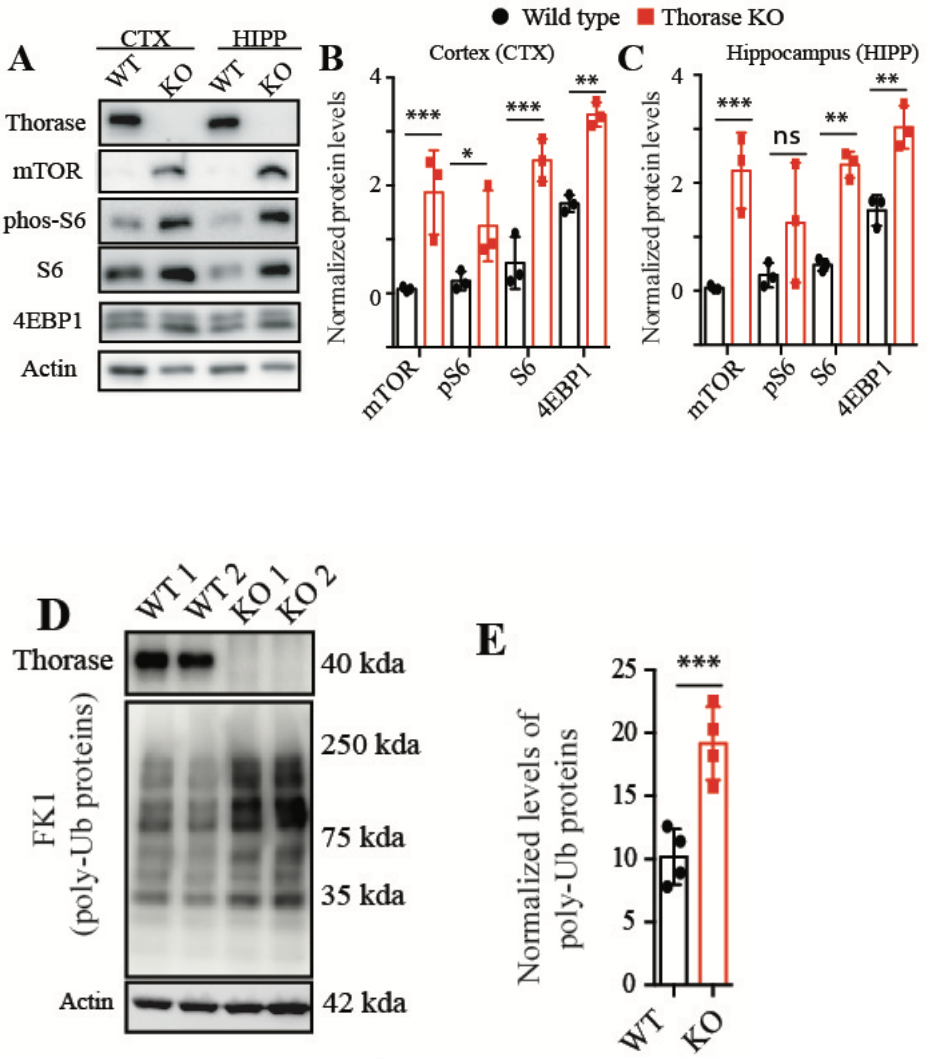

Figure 3-3. Thorase regulates the activity levels of the mTORC1 pathway. A, Immunoblot images of mTORC1-associated proteins in wildtype (WT) and Thorase knockout (KO) mouse brains. **B,** Quantification of samples from the cortex (CTX) in a (n = 3). **C,** Quantification of samples from the hippocampus (HIPP) in a (n = 3). **D,** Representative immunoblot images showing increased levels of poly-ubiquitinated (FK1) proteins in Thorase KO mice. **E,** Quantification of blots in D (n = 4).

Figure 3-4. Myelination levels are higher in Thorase knockout mice, and the mTOR inhibitor, rapamycin, ameliorates the phenotypes arising from the increased mTORC1 activation observed in the absence of Thorase.

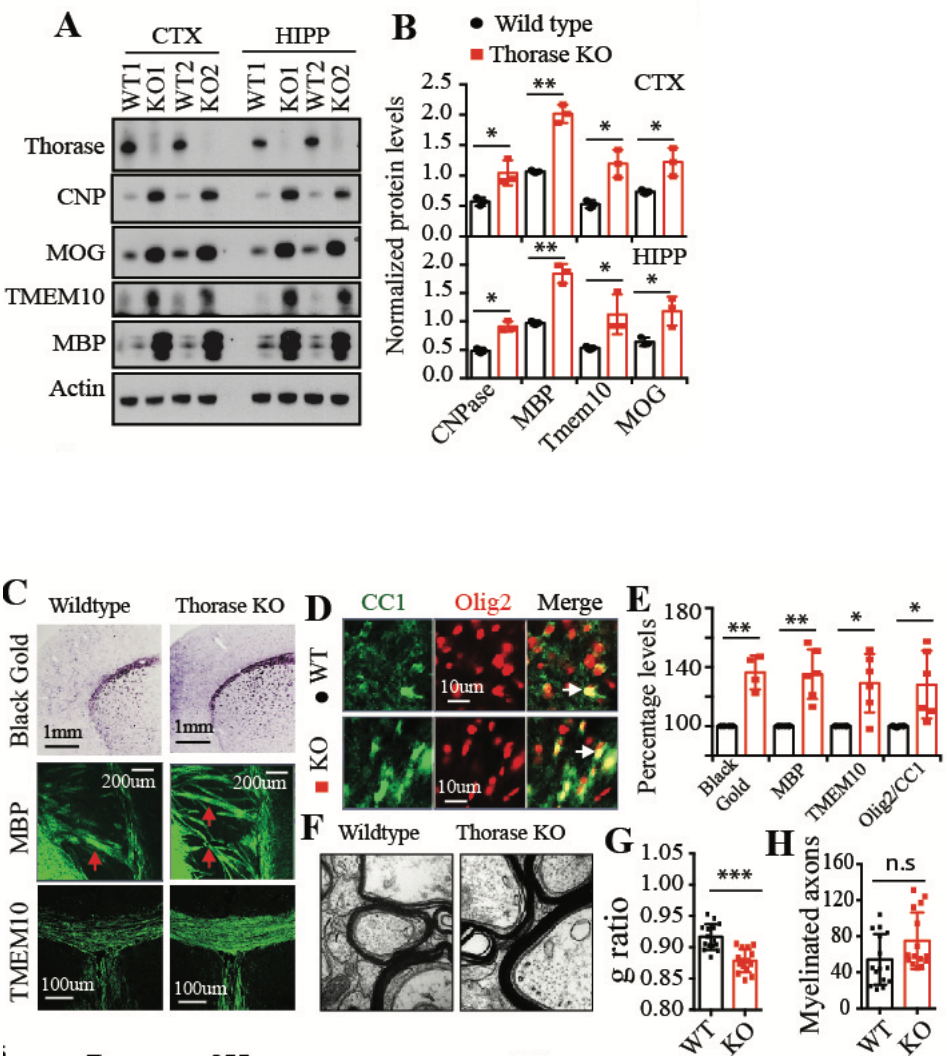

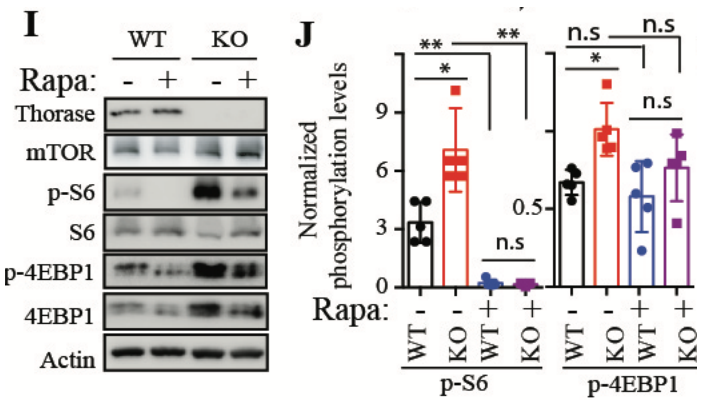
I
WT
KO
Rapa: - + - +
Thorase
mTOR
p-S6
S6
p-4EBP1
4EBP1
Actin
J
Normalized phosphorylation levels
**
**
*
n.s
n.s
*
n.s
9
6
3
0
0.5
Rapa: - - + +
WT KO WT KO
p-S6
p-4EBP1

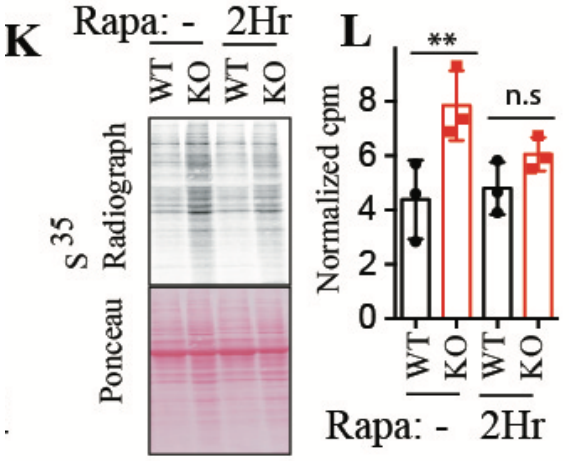
K
Rapa: - 2Hr
WT KO WT KO
S35 Radiograph
Ponceau
L
**
n.s
Normalized cpm
8
6
4
2
0
WT KO WT KO
Rapa: - 2Hr

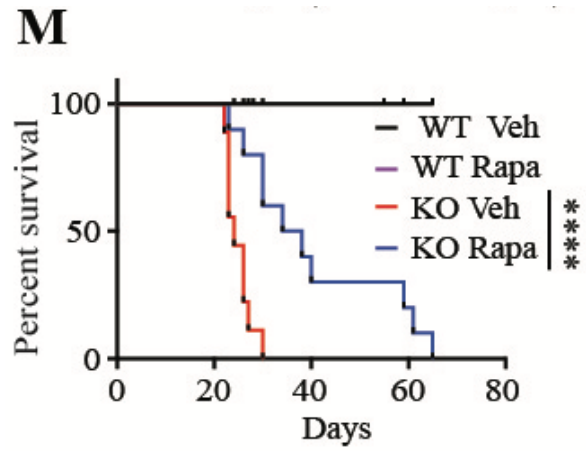
M
Percent survival
100
50
0
0 20 40 60 80
Days
WT Veh
WT Rapa
KO Veh
KO Rapa
***

Figure 3-4. Myelination levels are higher in Thorase knockout mice, and the mTOR inhibitor, rapamycin, ameliorates the phenotypes arising from the increased mTORC1 activation observed in the absence of Thorase. A, Immunoblot images of myelin proteins and oligodendrocyte markers in wildtype (WT) and Thorase knockout (KO) mouse brain lysates. **B**, Quantification of blots in a (n = 3). **C**, Representative images of myelin proteins, MBP, TMEM10 and black gold staining in mouse brain sections (fibers indicated by red arrows). **D**, Representative images of oligodendrocyte olig2/CC1 staining in mouse brain sections (double positive cells indicated by white arrows). **E**, Quantification of staining intensities of images from C and D (n = 6). **F**, Representative images of myelinated axons in the optic nerves. **G**, Graphical representation of myelin thickness (g ratio) of the optic nerves (n = 15). **H**, Quantification of number of myelinated axons (n = 15). **I**, Immunoblot images showing rapamycin (Rapa) treatment normalizes elevated mTORC1 activity in KO cells. **J**, Quantification of blots in I (n = 5). **K**, Representative images showing rapamycin inhibits increased protein synthesis in KO cells. **L**, Quantification of blots in J (n = 3). **M**, Survival curve of mice treated with rapamycin or vehicle (Veh) (Log Rank Mantel-Cox test, WT Veh n=12 ; WT Rapa n=9 ; KO Veh n=9 ; KO Rapa n=10; median survival KO Veh 24 days, KO Rapa 36 days). Data in B, E, G, H, J, L, M are mean ± standard error of the mean [SEM] of experiments performed, ****$p < 0.0001$, ***$p < 0.001$, **$p < 0.01$, *$p < 0.05$, n.s $p > 0.05$, ANOVA with Tukey-Kramer post-hoc test compared with WT or control.

Figure 3-5. Thorase interaction with mTOR is concomitant to a decrease in binding of mTOR to other mTORC1-related proteins (part II).

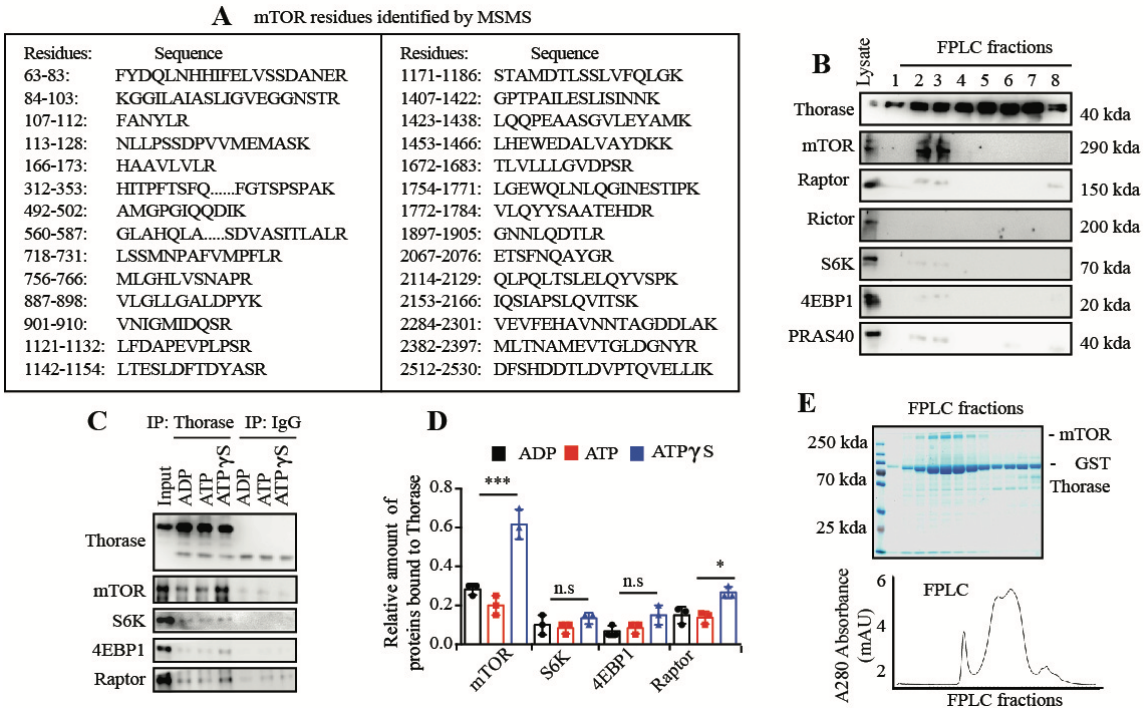

Figure 3-5. Thorase interaction with mTOR is concomitant to a decrease in binding of mTOR to other mTORC1-related proteins (part II). A, A list of mTOR peptides identified by mass spectrometry in Thorase pulldown. **B,** Immunoblots of FPLC fractions Thorase pulldown of mTOR. **C,** Immunoblot images of immunoprecipitation (IP) of Thorase in the presence of different nucleotides to pulldown mTORC1-associated proteins. **D,** Graphical representation of quantified blots in C (n = 3). **E,** Images of SDS-PAGE of FPLC fractions and FPLC profile confirming direct interaction of purified recombinant mTOR and GST-Thorase complex on FPLC size-exclusive column. Data in D are mean ± standard error of the mean [SEM] of experiments performed, ***$p < 0.001$, *$p < 0.05$, n.s $p > 0.05$, ANOVA with Tukey-Kramer post-hoc test compared with ADP.

Figure 3-6. Thorase disassembles the mTOR complex 1 (part II).

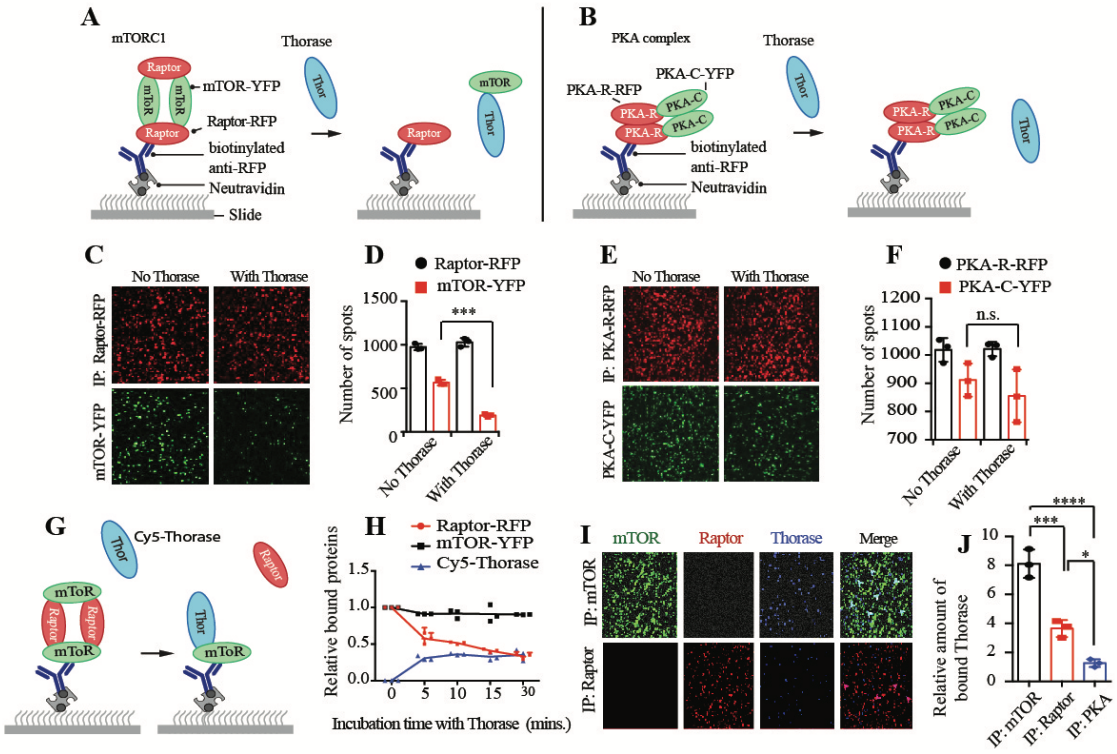

Figure 3-6. Thorase disassembles the mTOR complex 1 (part II). A, Schematic diagram of SiMPull analyses of mTOR-Raptor complex in the presence of Thorase. **B,** Schematic diagram of SiMPull analyses of PKA complex (control) in the presence of Thorase. **C,** Representative images from mTORC1 SiMPull confirming Thorase disassembles the mTOR-Raptor complex. **D,** Quantification of images in C (n = 3). **E,** Representative images from PKA SiMPull showing no significant disassembly of the control PKA complex in the presence of Thorase. **F,** Quantification of images in E (n = 3). **G,** Schematic diagram of mTOR-Pulldown SiMPull showing Thorase binds to mTOR upon disassembly of Raptor from mTORC1. **H,** Graphical representation of Raptor (red) disassociation from mTOR and Thorase (blue) binding to mTOR over time (n = 3, Thorase-Cy5 values 5x). **I,** Representative images of SiMPull binding analyses showing that Thorase has higher affinity for mTOR than Raptor. **J,** Graphical representation of quantified intensities from images in I. Data in D, F, H, J are mean ± standard error of the mean [SEM] of experiments performed, ****$p < 0.0001$, ***$p < 0.001$, *$p < 0.05$, n.s $p > 0.05$, ANOVA with Tukey-Kramer post-hoc test compared with control (no Thorase).

Figure 3-7. Thorase disassembly of the mTORC1 is ATP dependent.

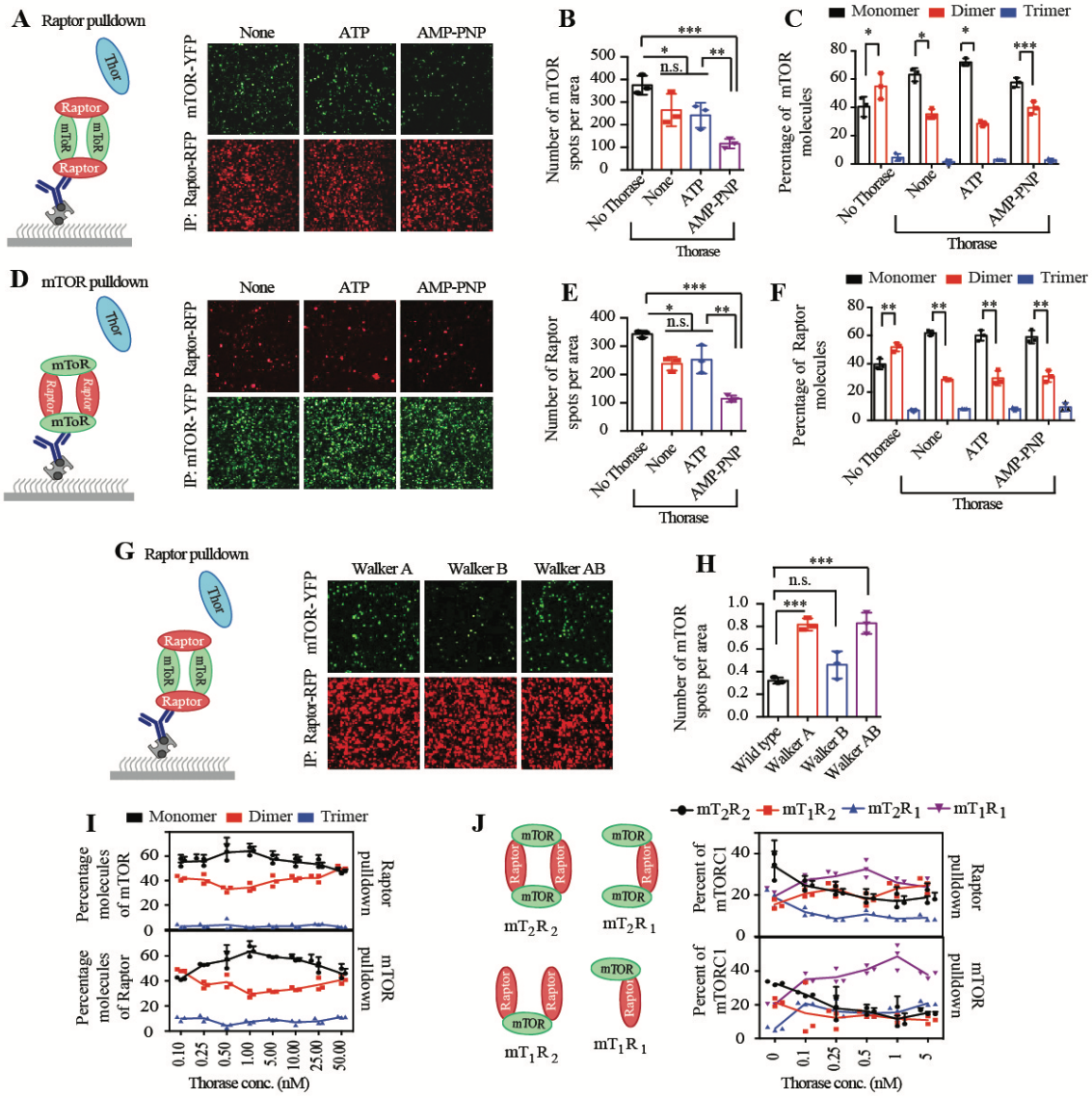

Figure 3-7. Thorase disassembly of the mTORC1 is ATP dependent. A, Schematic diagram and representative images of Raptor-pulldown SiMPull analyses of mTOR-Raptor complex in the presence of Thorase and different nucleotides. **B,** Quantification of number of mTOR spots per imaging area in a (n = 3). **C,** Quantification of the amount of different species of mTOR in the presence of Thorase and different nucleotides (n = 3). **D,** Schematic diagram and representative images of mTOR-pulldown SiMPull analyses of mTOR-Raptor complex in the presence of Thorase and different nucleotides. **E,** Quantification of number of Raptor spots per imaging area in D (n = 3). **F,** Quantification of the amount of different species of Raptor in the presence of Thorase and different nucleotides (n = 3). **G,** Schematic diagram and representative images of SiMPull analyses of mTOR-Raptor complex in the presence of different Thorase ATPase variants. **H,** Quantification of images in g showing Thorase ATP binding deficient variants, Walker A and AB do not significantly disassemble mTORC1 (n = 3). **I,** Graphical representation of the disassembly of different species of mTOR and Raptor in the presence of different concentrations of Thorase (n = 3). **J,** Schematic diagram and graphical representation of different complexes of mTORC1 in the presence of different concentrations of Thorase. Data in B, C, E, F, H, I, J are mean ± standard error of the mean [SEM] of experiments performed, ***$p < 0.001$, **$p < 0.01$, *$p < 0.05$, n.s $p > 0.05$, ANOVA with Tukey-Kramer post-hoc test compared with wildtype or control (no Thorase).

Figure 3-8. Thorase N-terminus is essential for the interaction with mTOR.

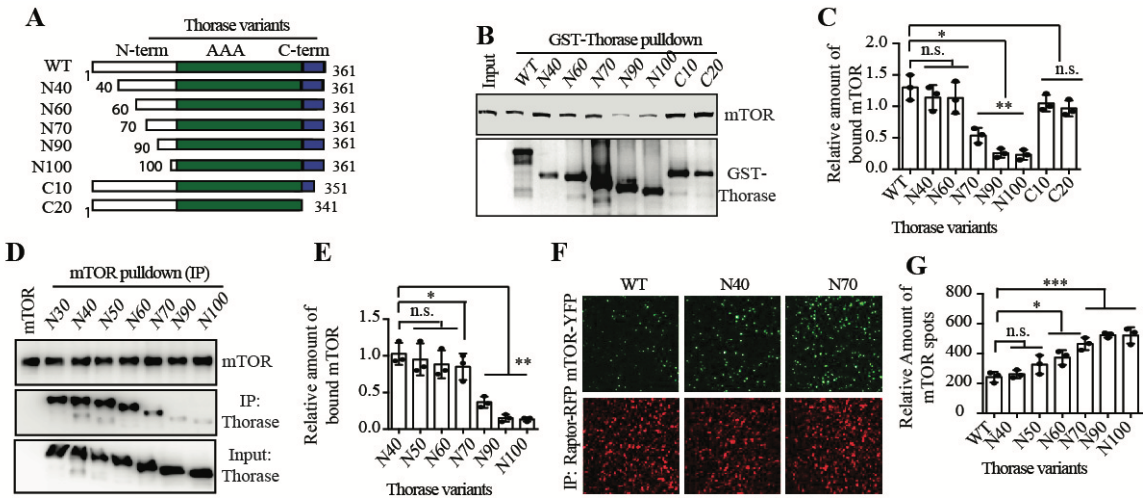

Figure 3-8. Thorase N-terminus is important for lysosomal localization. Fig. S4. Thorase N-terminus is essential for the interaction with mTOR. A, A schematic diagram of truncated variants of Thorase. **B,** Immunoblot images of different GST-Thorase truncated variants pulldown of mTOR. **C,** Quantification of blots in B (n = 3). **D,** Immunoblot images of mTOR pulldown of different Thorase truncated variants. **E,** Quantification of blots in D (n = 3). **F,** Representative images from Raptor-pulldown SiMPull in the presence of Thorase truncated variants. **G,** Quantification of signal intensities of images in f (n = 3). Data in C, E, G are mean ± standard error of the mean [SEM] of experiments performed, ***$p < 0.001$, **$p < 0.01$, *$p < 0.05$, n.s $p > 0.05$, ANOVA with Tukey-Kramer post-hoc test compared with WT.

Figure 3-9. mTORC1-related protein levels are elevated in Thorase knockout mice and fibroblasts.

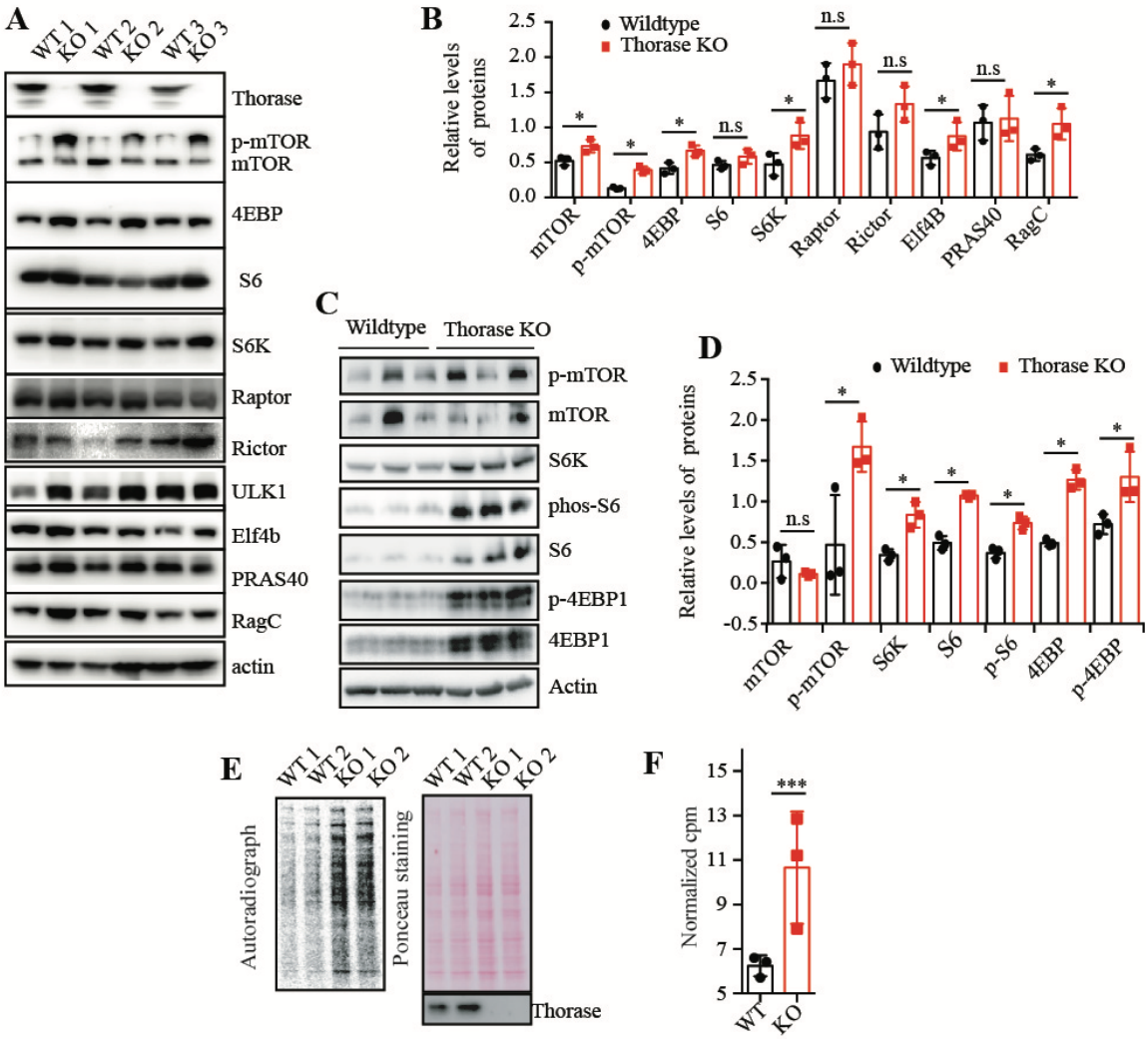

Figure 3-9. mTORC1-related protein levels are elevated in Thorase knockout mice and fibroblasts. A, Immunoblot images of mTORC1 protein expression in brain lysates of wildtype (WT) and Thorase knockout (KO) mice. **B,** Graphical representation of quantified blots in a (n = 3). **C,** Representative immunoblots mTORC1 protein expression in WT and KO mouse embryonic fibroblasts (MEFs). **D,** Quantification of blots in C (n = 3). **E,** Representative images showing increased protein synthesis in KO MEFs compared to WT MEFs. **F,** Graphical representation of blots in E (n = 3). Data in B, D, F are mean ± standard error of the mean [SEM] of experiments performed, ***$p < 0.001$, *$p < 0.05$, n.s $p > 0.05$, ANOVA with Tukey-Kramer post-hoc test compared with WT.

Figure 3-10. Increased myelination in Thorase knockout mice.

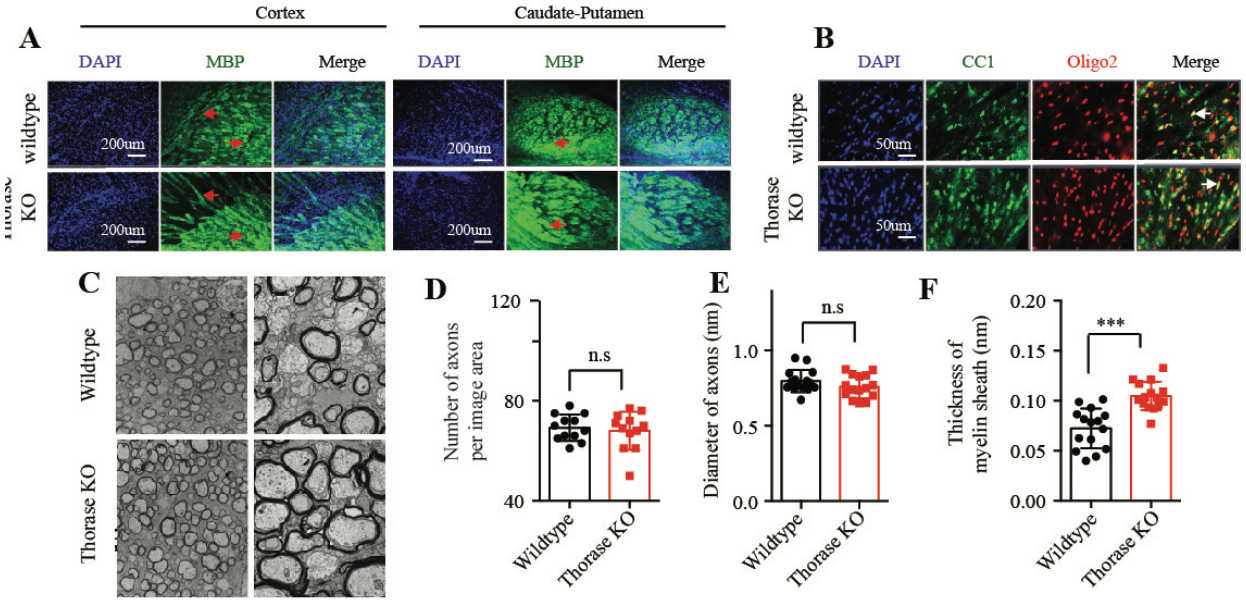

Figure 3-10. Increased myelination in Thorase knockout mice. A, Representative images of myelin basic protein (MBP) staining of different regions of the brain of wildtype (WT) and Thorase knockout (KO) mice. Increased myelin fibers in the cortex frontoparietalis as well as high levels of compact myelin fibers in the caudate-putamen (red arrows) of Thorase KO compared to wild type mice. **B,** Representative images of Oligo2/CC1 staining of the cortex of wildtype and Thorase KO mice (double positive cells indicated by white arrows). **C,** Representative images of optic nerves of wildtype and Thorase KO mice showing myelinated axons. **D,** Quantification of number of axons per image area of images in C (n = 12). **E,** Quantification of diameter of axons of images in c (n = 12). D, Quantification of number of myelin thickness of images in C (n = 12). mean ± standard error of the mean [SEM] of experiments performed, ***$p < 0.001$, n.s $p > 0.05$, ANOVA with Tukey-Kramer post-hoc test compared with wildtype.

Chapter 4. Future directions

The recent discovery of pathogenic variants that cause a recognizable neurological disease in newborns has given substantiation to the suspected importance of Thorase in protecting the brain. By uncovering an ever-increasing number of functions for Thorase, we are starting to understand that Thorase activity is required to ensure normal physiology in various cellular compartments. In particular, our study has revealed a new link between the survival and metabolism of neurons, which suggests that Thorase endows protection, at least partly, by maintaining neurons in a bioenergetically favorable state. While we have made commensurable progress in understanding the neuroprotective role of Thorase in the past few years, many intriguing questions remain to be answered that grant future research on Thorase.

Expression and activity of Thorase in different tissues and cell types, and regulation thereof

Zhang and colleagues first peeked into the relative expression of Thorase throughout the body (Zhang et al, 2011). They detected Thorase expression predominantly in the mouse brain and testis, with a high degree of expression variability in the brain. The striking neurological defects resulting from abnormal Thorase function in both mice and humans supports a prominent role of Thorase in the nervous system, with nuances. In mice, knocking out Thorase at the whole-body level leads to perinatal death, while animals with restricted Thorase deletion in the forebrain or midbrain are viable. This notion demonstrates the need for a more comprehensive analysis of Thorase actions in different brain cell types, including neuroglia. Generation of pertinent models using Thorase

lacking stem cells that can be differentiated into diverse cell types, or conditional knockout rodent models generated with inducible systems such as Cre-LoxP will enable to answer this fundamental question.

Along the same lines, it will be interesting to investigate how divergent levels of Thorase expression across tissues can be achieved, whether this is transcriptionally or translationally regulated or due to additional factors that modulate Thorase degradation. A particularly intriguing idea is that Thorase expression or localization within the cell is regulated by the intracellular levels of ATP, that is, that Thorase could behave or act in tandem with an ATP-sensing molecule. This could potentially tie the regulation of mTOR signaling with the metabolic status of the cell.

Furthermore, it will be insightful to understand whether any connection between different Thorase functions exist. For instance, mTORC1-dependent translation is required for synaptic plasticity, and mTORC1 has been suggested to regulate the surface expression of AMPAR (Wang et al, 2006). If in the absence of Thorase AMPAR endocytosis is impaired and excess mTORC1 activity leads to insertion of more AMPAR at the synapse, collectively this could explain the severe defects in neuronal excitability observed in mice and humans.

Substrate selection and recognition by Thorase

From studies with other AAA+ ATPases, it seems that cells can control one activity of a particular AAA+ protein without compromising other activities of the same AAA+

protein through the usage of adaptor proteins. The many protein adaptors known for p97 and the substrates they target p97 to exemplify this well (Stach & Freemont, 2017). It has been suggested that adaptor proteins tend to use a common platform, the N-terminal domain of AAA+ ATPases, for binding and regulating AAA+ activity.

Although a recent study in the yeast homolog of Thorase, Msp1, indicated that Msp1 alone could bind and extract mislocalized proteins from isolated liposomes (Wohlever et al, 2017), this *in vitro* study with isolated components hardly represents real cell physiology. Searching for adapters that shuttle Thorase to particular substrates in different subcellular localizations will be interesting and it will potentially explain whether Thorase exerts specialized functions in specific cell types, as regulation of adapter expression in a cell-dependent manner would allow for this. This same study suggested that Thorase recognizes exposed hydrophobic areas in their target proteins. Whether this is a generalizable substrate recognition mechanism for Thorase, or whether additional recognition motifs for it exist will help understand how Thorase operates and potentially bolster the discovery of additional substrates.

Structural insight into Thorase activity

Studies with the yeast homolog of Thorase, Msp1, have suggested that it oligomerizes into hexamers at the mitochondria (Wohlever et al, 2017). Whether Thorase also assembles into hexamers in mitochondria will be an important question to address. In addition, whether different Thorase functions are exerted by a common oligomeric conformation or whether functional specificity can stem from a diversification in Thorase

assembly is an idea worth testing. To answer this and other interesting questions, obtaining structural models of Thorase by nuclear magnetic resonance spectroscopy, X-ray crystallography and cryo-electron microscopy will be pivotal. Performing these structural studies with Thorase alone or in coordination with its substrates, and in the presence of different nucleotides, will be an important step towards understanding how Thorase binds substrates, how it transduces the energy of ATP hydrolysis and how it localizes to different cell compartments. The use of ATP binding or hydrolyzing mutants Walker A and B, and variants of Thorase associated with human disease will provide additional information about the structural nature of Thorase interactions and activities.

Investigation of the link between Thorase function and protein degradation

A recurrent observation made by several studies is that, in the absence of Thorase, certain proteins it regulates abnormally accumulate, suggesting that in physiological conditions Thorase may couple the disassembly of complexes or extraction of proteins with their degradation. It will be important to determine what cellular degradation pathways this activity depends upon, whether it is the ubiquitin-proteasome system, the autophagy machinery or whether Thorase associates with particular proteases. A feasible alternative is that, given mTOR blockade of autophagy, the accumulation of Thorase substrates observed in its absence may be a by-product of its failure to negatively regulate mTORC1 activity, which would involve a halt in autophagic flux. Genetically or pharmacologically ablating excess mTOR activity or inducing the activity of specific cellular degradation pathways could be a useful avenue to discern between all the above possibilities.

Phenotype-genotype relationship of emerging pathogenic Thorase variants

Any disruption in gene or protein sequence that disrupts protein function can provide enormous insight into the normal activity of a protein. Through comparative studies between wild type Thorase and its human pathogenic variants, and combining biochemical and structural techniques, these mutants will add a new dimension to our understanding on the function of Thorase. To establish a genotype-phenotype relationship for these variants, the generation of mouse models or stem cells that contain these familial mutations using CRISPR gene editing technology will be key. Insights from studies discussed earlier on the specificity of Thorase in different tissues or cell-types will be a guiding reference to evaluate whether these variants should be induced ubiquitously or whether their expression should be spatial- and temporally restricted.

References

Aggarwal, V., Ha, T. (2014). Single-molecule pull-down (SiMPull) for new-age biochemistry: methodology and biochemical applications of single-molecule pull-down (SiMPull) for probing biomolecular interactions in crude cell extracts. Bioessays. 36(11):1109-19. doi: 10.1002/bies.201400090.

Ahrens-Nicklas, R.C., Umanah, G.K.E., Sondheimer, N., Deardorff, M.A., Wilkens, A.B., Conlin, L.K., Santani, A.B., Nesbitt, A., Juulsola, J., Ma, E., Dawson, T.M., Dawson, V.L., Marsh, E.D. (2017). Precision therapy for a new disorder of AMPA receptor recycling due to mutations in ATAD1. Neurol Genet. 3(1): e130. doi: 10.1212/NXG.0000000000000130

Bar-Peled, L., Chantranupong, L., Cherniack, A.D., Chen, W.W., Ottina, K.A., Grabiner, B.C., Spear, E.D., Carter, S.L., Meyerson, M., Sabatini, D.M. (2013) A Tumor suppressor complex with GAP activity for the Rag GTPases that signal amino acid sufficiency to mTORC1. Science. 340(6136):1100-6. doi: 10.1126/science.1232044.

Baulac S. (2016). mTOR signaling pathway genes in focal epilepsies. Prog Brain Res. 226:61-79. doi: 10.1016/bs.pbr.2016.04.013.

Ben-Sahra, I., Hoxhaj, G., Ricoult, S.J.H., Asara, J.M., Manning, B.D. (2016) mTORC1 induces purine synthesis through control of the mitochondrial tetrahydrofolate cycle. Science. 2016 Feb 12;351(6274):728-733. doi: 10.1126/science.aad0489.

Brown, E.J., Albers, M.W., Shin, T.B., Ichikawa, K., Keith, C.T., Lane, W.S., Schreiber, S.L. (1994) A mammalian protein targeted by G1-arresting rapamycin-receptor complex. Nature. 369(6483):756-8. doi: 10.1038/369756a0

Chantranupong, L., Scaria, S.M., Saxton, R.A., Gygi, M.P., Shen, K., Wyant, G.A., Wang, T., Harper, J.W., Gygi, S.P., Sabatini, D.M. (2016) The CASTOR Proteins Are Arginine Sensors for the mTORC1 Pathway. Cell. 165(1):153-164. doi: 10.1016/j.cell.2016.02.035.

Chen, Y.C., Umanah, G.K., Dephoure, N., Andrabi, S.A., Gygi, S.P., Dawson, T.M., Dawson, V.L., Rutter, J. (2014). Msp1/ATAD1 maintains mitochondrial function by facilitating the degradation of mislocalized tail-anchored proteins. EMBO J. 33(14):1548-64. doi: 10.15252/embj.201487943.

Citraro, R., Leo, A., Constanti, A., Russo, E., De Sarro, G. mTOR pathway inhibition as a new therapeutic strategy in epilepsy and epileptogenesis. Pharmacol Res. 107:333-343. doi: 10.1016/j.phrs.2016.03.039.

Crino, P.B. (2015). mTOR signaling in epilepsy: insights from malformations of cortical development. Cold Spring Harb Perspect Med. 5(4). pii: a022442. doi: 10.1101/cshperspect.a022442.

Crino, PB. (2016). The mTOR signaling cascade: paving new roads to cure neurological disease. Nat Rev Neurol. 12(7):379-92. doi: 10.1038/nrneurol.2016.81.

Dai, C., Liang, D., Li, H., Sasaki, M., Dawson, T.M., Dawson, V.L. (2010). Functional identification of neuroprotective molecules. PLoS One. 5(11):e15008. doi: 10.1371/journal.pone.0015008.

Dibble, C.C., Manning, B.D. (2013) Signal integration by mTORC1 coordinates nutrient input with biosynthetic output. Nat Cell Biol. 2013 Jun; 15(6): 555–564. doi: 10.1038/ncb2763

Egan, D., Kim, J., Shaw, R.J., Guan, K.L. The autophagy initiating kinase ULK1 is regulated via opposing phosphorylation by AMPK and mTOR. Autophagy. 7(6):643-4. Autophagy 7, 643–644 (2011). doi: 10.4161/auto.7.6.15123

Eng, C.P., Sehgal, S.N., Vézina, C. (1984). Activity of rapamycin (AY-22,989) against transplanted tumors. J Antibiot (Tokyo) 37:1231–1237. doi: 10.7164/antibiotics.37.1231

Evans, K.J., Gomes, E.R., Reisenweber, S.M., Gundersen, G.G., Lauring, B.P. (2005) Linking axonal degeneration to microtubule remodeling by Spastin-mediated microtubule severing. J Cell Biol. 168(4):599-606. doi: 10.1083/jcb.200409058

Gidday, J.M. (2006) Cerebral preconditioning and ischaemic tolerance. Nat Rev Neurosci. 7(6):437-48. doi:10.1038/nrn1927

Goodchild, R.E., Dauer, W.T. (2004) Mislocalization to the nuclear envelope: an effect of the dystonia-causing torsinA mutation. Proc Natl Acad Sci U S A. 101(3):847-52. doi: 10.1073/pnas.0304375101

Gu, X., Orozco, J.M., Saxton, R.A., Condon, K.J., Liu, G.Y., Krawczyk, P.A., Scaria, S.M., Harper, J.W., Gygi, S.P., Sabatini, D.M. (2017) SAMTOR is an S-adenosylmethionine sensor for the mTORC1 pathway. Science. 358(6364):813-818. doi: 10.1126/science.aao3265.

Hara, K., Maruki, Y., Long, X., Yoshino, K., Oshiro, N., Hidayat, S., Tokunaga, C., Avruch, J., Yonezawa K. (2002) Raptor, a binding partner of target of rapamycin (TOR), mediates TOR action. Cell. 110(2):177-89. doi: 10.1016/S0092-8674(02)00833-4

Hegde, R.S. (2014) Msp1: patrolling mitochondria for lost proteins. EMBO J. 33(14):1509-10. doi: 10.15252/embj.201488930.

Heitman, J., Movva, N.R., Hall, M.N. (1991). Targets for cell cycle arrest by the immunosuppressant rapamycin in yeast. Science. 253(5022):905-9. doi: 10.1126/science.1715094

Iadevaia, V., Liu, R., Proud, C.G. (2014). mTORC1 signaling controls multiple steps in ribosome biogenesis. Semin Cell Dev Biol. 36:113-20. doi: 10.1016/j.semcdb.2014.08.004.

Jain, A., Arauz, E., Aggarwal, V., Ikon, N., Chen, J., Ha, T. (2014) Stoichiometry and assembly of mTOR complexes revealed by single-molecule pulldown. Proc Natl Acad Sci U S A. 111(50):17833-8. doi: 10.1073/pnas.1419425111.

Jain, A., Liu, R., Ramani, B., Arauz, E., Ishitsuka, Y., Ragunathan, K., Park, J., Chen, J., Xiang, Y.K., Ha, T. (2011) Probing cellular protein complexes using single-molecule pull-down. Nature. 473(7348):484-8. doi: 10.1038/nature10016.

Johnson, J.O., Mandrioli, J., Benatar, M., Abramzon, Y., Van Deerlin, V.M., Trojanowski, J.Q., Gibbs, J.R., Brunetti, M., Gronka, S., Wuu, J., Ding, J., McCluskey, L., Martinez-Lage, M., Falcone, D., Hernandez, D.G., Arepalli, S., Chong, S., Schymick, J.C., Rothstein, J., Landi, F., Wang, Y.D., Calvo, A., Mora, G., Sabatelli, M., Monsurrò, M.R., Battistini, S., Salvi, F., Spataro, R., Sola, P., Borghero, G.; ITALSGEN Consortium, Galassi, G., Scholz, S.W., Taylor, J.P., Restagno, G., Chiò, A., Traynor, B.J. (2010) Exome sequencing reveals VCP mutations as a cause of familial ALS. Neuron. 68(5):857-64. doi: 10.1016/j.neuron.2010.11.036.

Kim, D.H., Sarbassov, D.D., Ali, S.M., King, J.E., Latek, R.R., Erdjument-Bromage, H., Tempst, P., Sabatini. D.M. (2002) mTOR interacts with raptor to form a nutrient-sensitive complex that signals to the cell growth machinery. Cell. 110(2):163-75. doi: 10.1016/S0092-8674(02)00808-5

Koltin, Y., Faucette, L., Bergsma, D.J., Levy, M.A., Cafferkey, R., Koser, P.L., Johnson, R.K., Livi, G.P. (1991). Rapamycin sensitivity in Saccharomyces cerevisiae is mediated by a peptidyl-prolyl cis-trans isomerase related to human FK506-binding protein. Mol Cell Biol. 11(3):1718-23. doi: 10.1128/MCB.11.3.1718

Li, L., Zheng, J., Wu, X., Jiang, H. (2019) Mitochondrial AAA-ATPase Msp1 detects mislocalized tail-anchored proteins through a dual-recognition mechanism. EMBO Rep. 20(4). pii: e46989. doi: 10.15252/embr.201846989.

Lipton, J.O, Sahin, M. (2014) The Neurology of mTOR. Neuron. 2014 Oct 22; 84(2): 275–291. doi: 10.1016/j.neuron.2014.09.034.

Liu, Y., Yagita, Y., Fujiki, Y. (2016). Assembly of Peroxisomal Membrane Proteins via the Direct Pex19p-Pex3p Pathway. Traffic.17(4):433-55. doi: 10.1111/tra.12376.

Ma, X., Blenis, J. (2009). Molecular mechanisms of mTOR-mediated translational control. Nat Rev Mol Cell Biol. 10(5):307-18. doi: 10.1038/nrm2672.

Martel, R.R., Klicius, J., Galet, S. (1977). Inhibition of the immune response by rapamycin, a new antifungal antibiotic. Can J Physiol Pharmacol 55:48–51. doi: 10.1139/y77-007

Menon, S., Dibble, C.C., Talbott, G., Hoxhaj, G., Valvezan, A.J., Takahashi, H., Cantley, L.C,, Manning, B.D. (2014) Spatial control of the TSC complex integrates insulin

and nutrient regulation of mTORC1 at the lysosome. Cell. 156(4):771-85. doi: 10.1016/j.cell.2013.11.049.

Miller, J.M., Enemark, E.J. (2016). Fundamental Characteristics of AAA+ Protein Family Structure and Function. Archaea. 2016:9294307. doi:10.1155/2016/9294307

Moretto, E., Passafaro, M. (2018). Recent Findings on AMPA Receptor Recycling. Front Cell Neurosci. 12:286. doi: 10.3389/fncel.2018.00286.

Okreglak, V., Walter, P. (2014). The conserved AAA-ATPase Msp1 confers organelle specificity to tail-anchored proteins. Proc Natl Acad Sci U S A. 111(22):8019-24. doi: 10.1073/pnas.1405755111.

Panchaud, N., Péli-Gulli, M.P., De Virgilio, C. (2013) Amino acid deprivation inhibits TORC1 through a GTPase-activating protein complex for the Rag family GTPase Gtr1. Sci Signal. 6(277):ra42. doi: 10.1126/scisignal.2004112.

Peña-Llopis, S., Vega-Rubin-de-Celis, S., Schwartz, J.C., Wolff, N.C., Tran, T.A., Zou, L., Xie, X.J., Corey, D.R., Brugarolas, J. (2011). Regulation of TFEB and V-ATPases by mTORC1. EMBO J. 30(16):3242-58. doi: 10.1038/emboj.2011.257.

Piard, J., Umanah, G.K.E., Harms, F.L., Abalde-Atristain, L., Amram, D., Chang, M., Chen, R., Alawi, M., Salpietro, V., Rees, M.I., Chung, S.K., Houlden, H., Verloes, A., Dawson, T.M., Dawson, V.L., Van Maldergem, L., Kutsche, K. (2018) A homozygous ATAD1 mutation impairs postsynaptic AMPA receptor trafficking and causes a lethal encephalopathy. Brain. 141(3):651-661. doi: 10.1093/brain/awx377.

Pignatelli, M., Umanah, G.K.E., Ribeiro, S.P., Chen, R., Karuppagounder, S.S., Yau, H.J., Eacker, S., Dawson, V.L, Dawson, T.M., Bonci, A. (2017) Synaptic Plasticity onto Dopamine Neurons Shapes Fear Learning. Neuron. 93(2):425-440. doi: 10.1016/j.neuron.2016.12.030.

Porstmann, T., Santos, C.R., Griffiths, B., Cully, M., Wu, M., Leevers, S., Griffiths, J.R., Chung, Y.L., Schulze, A. (2008). SREBP Activity Is Regulated by mTORC1 and Contributes to Akt-Dependent Cell Growth. Cell Metab. 8(3-3): 224–236. doi: 10.1016/j.cmet.2008.07.007

Prendergast, J., Umanah, G.K., Yoo, S.W., Lagerlöf, O., Motari, M.G., Cole, R.N., Huganir, R.L., Dawson, T.M., Dawson, V.L., Schnaar, R.L. (2014). Ganglioside regulation of AMPA receptor trafficking. J Neurosci. 34(39):13246-58. doi: 10.1523/JNEUROSCI.1149-14.2014.

Reuber, B.E., Germain-Lee, E., Collins, C.S., Morrell, J.C., Ameritunga, R., Moser, H.W., Valle, D., Gould, S.J. (1997) Mutations in PEX1 are the most common cause of peroxisome biogenesis disorders. Nat Genet. 17(4):445-8.doi: 10.1038/ng1297-445

Robitaille, A.M., Christen, S., Shimobayashi, M., Cornu, M., Fava, L.L., Moes, S., Prescianotto-Baschong, C., Sauer, U., Jenoe, P., Hall, M.N. (2013). Quantitative phosphoproteomics reveal mTORC1 activates de novo pyrimidine synthesis. Science. 339(6125):1320-3. doi: 10.1126/science.1228771.

Sabatini, D.M., Erdjument-Bromage, H., Lui, M., Tempst, P., Snyder, S.H. (1994) RAFT1: a mammalian protein that binds to FKBP12 in a rapamycin-dependent

fashion and is homologous to yeast TORs. Cell.78(1):35-43. doi: 10.1016/0092-8674(94)90570-3

Sabatini, D.M. (2017) Twenty-five years of mTOR: Uncovering the link from nutrients to growth. Proc Natl Acad Sci U S A. 114(45):11818-11825. doi:10.1073/pnas.1716173114.

Sabers, C.J., Martin, M.M., Brunn, G.J., Williams, J.M., Dumont, F.J., Wiederrecht, G., Abraham, R.T. (1995) Isolation of a protein target of the FKBP12-rapamycin complex in mammalian cells. J Biol Chem. 270(2):815-22. doi: 10.1074/jbc.270.2.815

Sancak, Y., Peterson, T.R., Shaul, Y.D., Lindquist, R.A., Thoreen, C.C., Bar-Peled, L., Sabatini, D.M. (2008) The Rag GTPases bind raptor and mediate amino acid signaling to mTORC1. Science. 320(5882):1496-501. doi: 10.1126/science.1157535.

Sancak, Y., Bar-Peled, L., Zoncu, R., Markhard, A.L., Nada, S., Sabatini, D.M. (2010) Ragulator-Rag complex targets mTORC1 to the lysosomal surface and is necessary for its activation by amino acids. Cell. 141(2):290-303. doi: 10.1016/j.cell.2010.02.024.

Sarbassov, D.D., Ali, S.M., Kim, D.H., Guertin, D.A., Latek, R.R., Erdjument-Bromage, H., Tempst, P., Sabatini, D.M. (2004) Rictor, a novel binding partner of mTOR, defines a rapamycin-insensitive and raptor-independent pathway that regulates the cytoskeleton. Curr Biol. 14(14):1296-302. doi: 10.1016/j.cub.2004.06.054

Saxton, R.A., Sabatini D.M. (2017) mTOR Signaling in Growth, Metabolism, and Disease. Cell. 168(6):960-976. doi: 10.1016/j.cell.2017.02.004.

Stach, L., Freemont, P.S. (2017). The AAA+ ATPase p97, a cellular multitool. Biochem J. 474(17): 2953–2976. doi: 10.1042/BCJ20160783

Sysoeva, T.A. (2017). Assessing heterogeneity in oligomeric AAA+ machines. Cell Mol Life Sci. 74(6):1001-1018. doi: 10.1007/s00018-016-2374-z.

Tang, W.K., Xia, D. (2016). Mutations in the Human AAA+ Chaperone p97 and Related Diseases. Front Mol Biosci. 3:79. doi: 10.3389/fmolb.2016.00079

Umanah, G.K.E., Pignatelli, M., Yin, X., Chen, R., Crawford, J., Neifert, S., Scarffe, L., Behensky, A.A., Guiberson, N., Chang. M., Ma, E., Kim, J.W., Castro, C.C., Mao. X., Chen, L,, Andrabi, S.A., Pletnikov, M.V., Pulver, A.E., Avramopoulos, D., Bonci, A., Valle, D., Dawson, T.M., Dawson, V.L. (2017) Thorase variants are associated with defects in glutamatergic neurotransmission that can be rescued by Perampanel. Sci Transl Med. 9(420). pii: eaah4985. doi: 10.1126/scitranslmed.aah4985.

Valvezan, A.J., Manning, B.D. (2019) Molecular logic of mTORC1 signaling as a metabolic rheostat. Nature Metabolism 1:321–333. doi: 10.1038/s42255-019-0038-7

Vézina, C., Kudelski, A., Sehgal, S.N. (1975). Rapamycin (AY-22,989), a new antifungal antibiotic. I. Taxonomy of the producing streptomycete and isolation of the active principle. J Antibiot (Tokyo) 28:721–726. doi: 10.7164/antibiotics.28.721

Wang, Y., Barbaro, M.F., Baraban, S.C. (2006). A role for the mTOR pathway in surface expression of AMPA receptors. Neurosci Lett. 401(1-2):35-9 doi: 10.1016/j.neulet.2006.03.011

Wohlever, M.L., Mateja, A., McGilvray, P.T., Day, K.J., Keenan, R.J. (2017). Msp1 Is a Membrane Protein Dislocase for Tail-Anchored Proteins. Mol Cell. 67(2):194-202.e6. doi: 10.1016/j.molcel.2017.06.019.

Wolf, N.I, Zschocke, J., Jakobs, C, Rating, D., Hoffmann, GF. (2018). ATAD1 encephalopathy and stiff baby syndrome: a recognizable clinical presentation. Brain. 141(6):e49. doi: 10.1093/brain/awy095.

Wolfson, R.L., Chantranupong, L., Saxton, R.A., Shen, K., Scaria, S.M., Cantor, J.R., Sabatini, D.M. (2016) Sestrin2 is a leucine sensor for the mTORC1 pathway. Science. 351(6268):43-8. doi: 10.1126/science.aab2674.

Wolfson, R.L., Chantranupong, L., Wyant, G.A., Gu, X., Orozco, J.M., Shen, K., Condon, K.J., Petri, S., Kedir, J., Scaria, S.M., Abu-Remaileh, M., Frankel, W.N., Sabatini, D.M. (2017) KICSTOR recruits GATOR1 to the lysosome and is necessary for nutrients to regulate mTORC1. Nature. 543(7645):438-442. doi: 10.1038/nature21423.

Yang, H., Jiang, X., Li, B., Yang, H.J., Miller, M., Yang, A., Dhar, A., Pavletich, N.P. (2017) Mechanisms of mTORC1 activation by RHEB and inhibition by PRAS40. Nature. 552(7685):368-373. doi: 10.1038/nature25023.

Zhang, J., Wang, Y., Chi, Z., Keuss, M.J., Pai, Y.M., Kang, H.C., Shin, J.H., Bugayenko, A., Wang, H., Xiong, Y., Pletnikov, M.V., Mattson, M.P., Dawson, T.M., Dawson, V.L. (2011). The AAA+ ATPase Thorase regulates AMPA receptor-dependent synaptic plasticity and behavior. Cell. 145(2):284-99. doi: 10.1016/j.cell.2011.03.016.

Zou, J., Zhou, L., Du, X.X., Ji, Y., Xu, J., Tian, J., Jiang, W., Zou, Y., Yu, S., Gan, L., Luo, M., Yang, Q., Cui, Y., Yang, W., Xia, X., Chen, M., Zhao, X., Shen, Y., Chen, P.Y., Worley, P.F., Xiao, B. (2011) Rheb1 is required for mTORC1 and myelination in postnatal brain development. Dev Cell. 2011 Jan 18;20(1):97-108. doi: 10.1016/j.devcel.2010.11.020.

'HH7=AE;76)

Order Completed

Thank you for your order.

This Agreement between Miss. Leire Abalde-Atristain ("You") and Oxford University Press ("Oxford University Press") consists of your license details and the terms and conditions provided by Oxford University Press and Copyright Clearance Center.

Your confirmation email will contain your order number for future reference.

printable details

License Number	4567130000499
License date	Apr 13, 2019
Licensed Content Publisher	Oxford University Press
Licensed Content Publication	Brain
Licensed Content Title	A homozygous *ATAD1* mutation impairs postsynaptic AMPA receptor trafficking and causes a lethal encephalopathy
Licensed Content Author	Piard, Juliette; Umanah, George K Essien
Licensed Content Date	Jan 30, 2018
Licensed Content Volume	141
Licensed Content Issue	3
Type of Use	Thesis/Dissertation
Requestor type	Author of this OUP content
Format	Electronic
Portion	Figure/table
Number of figures/tables	1
Will you be translating?	No
Title	Metabolic Dysregulation in Neurodevelopment and Neurodegeneration
Institution name	n/a
Expected presentation date	May 2019
Portions	Figure 2 and Figure 3A-B
Requestor Location	Miss. Leire Abalde-Atristain 11 East Chase BALTIMORE, MD 21202 United States Attn: Miss. Leire Abalde-Atristain

)

#

HI

Publisher Tax ID	GB125506730
Total	0.00 USD

ORDER MORE CLOSE WINDOW

Copyright clearance:

I-Hsun Wu hereby grants Leire Abalde-Atristain permission to use the figures below in her Ph.D. dissertation:

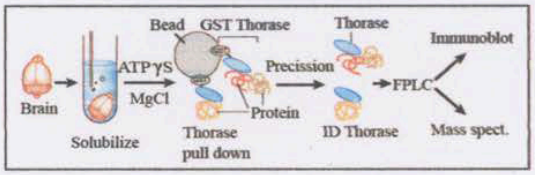

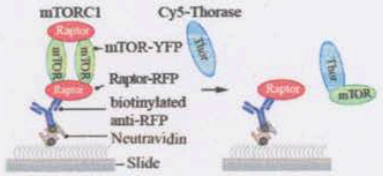

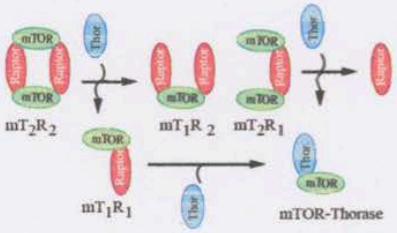

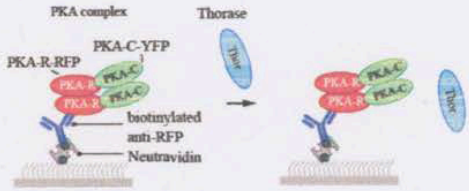

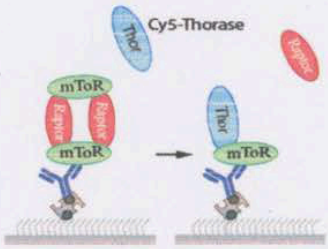

April 23rd, 2019

Wu, I-Hsun 吳怡勳

I-Hsun Wu, MA, CMI
Research Associate (Scientific and Medical Illustrator)
Johns Hopkins University School of Medicine
Institute for Cell Engineering

Curriculum Vitae

CURRICULUM VITAE FOR Ph.D. CANDIDATES

The Johns Hopkins University School of Medicine

Leire Abalde-Atristain	May 20, 2019
Name	Date of this Version

Educational History:

Ph.D. expected	2019	Program in Cellular and Molecular Medicine Johns Hopkins University School of Medicine Mentors: Valina L. Dawson, Ph.D. and Ted M. Dawson, M.D., Ph.D.
M.S.	2012	Biomedical Research Pompeu Fabra University, Barcelona, Spain
B.S.	2011	Biotechnology Autonomous University of Barcelona, Spain

Other Professional Experience:

Research Rotation	2014	Laboratory of Dr. Linzhao Chen, Ph.D. Johns Hopkins University School of Medicine
Research Rotation	2013	Laboratory of Dr. Hongjun Song, Ph.D. Johns Hopkins University School of Medicine
Graduate Research Assistant	2011-2012	Laboratory of Dr. Izpisua-Belmonte, Ph.D. Center of Regenerative Medicine in Barcelona
Summer Intern	2010	Laboratory of Dr. García Martín, Ph.D. Inbiomed Foundation, San Sebastian, Spain

Scholarships:

Pollard Scholarship	2014	Johns Hopkins University Stipend Support ($500)

Doctoral Scholarship	2013-2015	La Caixa Foundation, Spain Stipend Support ($30,000/year) and tuition support (full tuition)
Undergraduate Scholarship	2007	Government of Spain Tuition Support (full tuition)

Honors:

2019	Martin and Carol Macht Research Award	The 42nd Young Investigator's Day, Johns Hopkins University School of Medicine
2018	Poster Award, 1st place	Solomon H. Snyder Department of Neuroscience Retreat, Johns Hopkins University School of Medicine

Peer-reviewed Publications:

Abalde-Atristain L. (2019) Editor's Choice: GALvanizing Alzheimer's disease therapy to combat the inflamed brain. Sci Transl Med. 11(491).

Abalde-Atristain L. (2019) Editor's Choice: Neuronal connections killed in cold blood. Sci Transl Med. 11(481).

Piard J, Umanah GKE, Harms FL, **Abalde-Atristain L**, Amram D, Chang M, Chen R, Alawi M, Salpietro V, Rees MI, Chung SK, Houlden H, Verloes A, Dawson TM, Dawson VL, Van Maldergem L, Kutsche K. (2018) A homozygous ATAD1 mutation impairs postsynaptic AMPA receptor trafficking and causes a lethal encephalopathy. Brain. 141(3):651-661.

Piard J, Essien Umanah GK, Harms FL, **Abalde-Atristain L**, Amram D, Chang M, Chen R, Alawi M, Salpietro V, Rees MI, Chung SK, Houlden H, Verloes A, Dawson TM, Dawson VL, Van Maldergem L, Kutsche K. (2018) Reply: ATAD1 encephalopathy and stiff baby syndrome: a recognizable clinical presentation. Brain. 141(6):e50.

Smith C, **Abalde-Atristain L**, He C, Brodsky BR, Braunstein EM, Chaudhari P, Jang YY, Cheng L and Ye Z. (2015) Efficient and allele-specific genome editing of disease loci in human iPSCs. Mol Ther. 23(3):570-7.

Martin I, **Abalde-Atristain L**, Kim JW, Dawson TM, Dawson VL. Aberrant Protein Synthesis in G2019S LRRK2 Drosophila Parkinson's Disease-Related Phenotypes. (2014) Fly (Austin). 8(3):165-9.

Smith C, Gore A, Yan W, **Abalde-Atristain L**, Li Z, He C, Wang Y, Brodsky RA, Zhang K, Cheng L, Ye Z. (2014) Whole genome sequencing analysis reveals high specificity of CRISPR/Cas9 and TALEN based genome editing in human iPSCs. Cell Stem Cell. 15(1):12-3.

Chapters:

Kim JW, **Abalde-Atristain L**, Jia H, Dawson VL, Dawson TM. (2017) Protein translation in Parkinson's disease. In: Verstreken P, Ed., Parkinson's Disease: Molecular Mechanisms Underlying Pathology. San Diego: Academic Press. 281-309.

Presentations:

Essien Umanah GK and **Abalde-Atristain L**, Mitra J, Yu Z, Chang M, Tangella K, Chen R, Delannoy M, Aggarwal V, Xiao B, Worley P, Ha T, Dawson TM and Dawson VL. AAA+ ATPase Thorase Regulates mTOR Signaling Through the Disassembly of the mTOR Complex 1. CSHL Nutrient Signaling Meeting, Cold Spring Harbor, NY, October, 2018.

Essien Umanah GK and **Abalde-Atristain L**, Mitra J, Yu Z, Chang M, Tangella K, Chen R, Delannoy M, Aggarwal V, Xiao B, Worley P, Ha T, Dawson TM and Dawson VL. AAA+ ATPase Thorase Regulates mTOR Signaling Through the Disassembly of the mTOR Complex 1. The Physics of Living Systems Symposium at Johns Hopkins University, Baltimore, MD, August, 2018.

Essien Umanah GK and **Abalde-Atristain L**, Mitra J, Yu Z, Chang M, Tangella K, Chen R, Delannoy M, Aggarwal V, Xiao B, Worley P, Ha T, Dawson TM and Dawson VL. AAA+ ATPase Thorase Regulates mTOR Signaling Through the Disassembly of the mTOR Complex 1. Spring Baltimore Brain Series at the National Institute on Drug and Abuse, Baltimore, MD, April, 2018.

Service and Leadership:

2019 Poster Judge, 2nd annual Women in STEM Symposium
Johns Hopkins University

2019	Member, Baltimore Brain Series Organizing Committee, Baltimore
2018	Member, Greater Baltimore Society for Neuroscience Steering Committee, Baltimore
2018	Volunteer, Science Outside the Lines Program Johns Hopkins University
2018	Invited speaker, Health Professions Across the Curriculum Day Johns Hopkins University
2018	Volunteer, Brain Awareness Week, Baltimore
2018	Member, CASSS and Johns Hopkins Pharma and Biotech Industry Mentorship Program Steering Committee
2018	Instructor of Anatomy and Physiology, Johns Hopkins University
2017-2018	Co-president, Hopkins Biotech Network
2017	Outreach Volunteer, BrainFest, Baltimore MD
2017	Curriculum developer for Project EVOLVE Johns Hopkins University School of Medicine
2016	Tutor of Biostatistics, Johns Hopkins University School of Medicine
2014	Teaching Assistant of Molecular Biology and Genomics Johns Hopkins University School of Medicine